A SAMPLE EFFICIENT ALTERNATING MINIMIZATION-BASED ALGORITHM FOR ROBUST PHASE RETRIEVAL

Adarsh Barik
Institute of Data Science
National University of Singapore
Singapore, 117602
abarik@nus.edu.sg

Anand Krishna
Department of Electrical and Computer Engineering
National University of Singapore
Singapore, 117583
akr@nus.edu.sg

Vincent Y. F. Tan
Department of Mathematics
Department of Electrical and Computer Engineering
National University of Singapore
Singapore, 119077
vtan@nus.edu.sg

ABSTRACT

In this work, we study the robust phase retrieval problem where the task is to recover an unknown signal $\boldsymbol{\theta}^* \in \mathbb{R}^d$ in the presence of potentially arbitrarily corrupted magnitude-only linear measurements. We propose an alternating minimization approach that incorporates an oracle solver for a non-convex optimization problem as a subroutine. Our algorithm guarantees convergence to $\boldsymbol{\theta}^*$ and provides an explicit polynomial dependence of the convergence rate on the fraction of corrupted measurements. We then provide an efficient construction of the aforementioned oracle under a sparse arbitrary outliers model and offer valuable insights into the geometric properties of the loss landscape in phase retrieval with corrupted measurements. Our proposed oracle avoids the need for computationally intensive spectral initialization, using a simple gradient descent algorithm with a constant step size and random initialization instead. Additionally, our overall algorithm achieves nearly linear sample complexity, $\mathcal{O}(d \operatorname{polylog}(d))$.

1 Introduction

The problem of phase retrieval consists of recovering an unknown target signal from intensity-only measurements. It has gained wide interest in many areas of engineering, applied physics, and machine learning (Dong et al., 2023), such as optics (Walther, 1963), X-ray crystallography (Millane, 1990), inference of DNA structure (Stefik, 1978), and more. Mathematically, the task is to learn an unknown signal $\boldsymbol{\theta}^* \in \mathbb{R}^d$ from n magnitude-only linear measurements[1]. To ensure the smoothness of the loss function, we describe the data generation process of the phase retrieval problem in the following quadratic form:

$$y_i = \langle \boldsymbol{x}_i, \boldsymbol{\theta}^* \rangle^2, \quad i \in [n], \tag{1}$$

where $[n]$ is a shorthand to denote the set $\{1, \ldots, n\}$. Borrowing terminology from linear regression literature (Bakshi and Prasad, 2021), we term $\boldsymbol{x}_i \in \mathbb{R}^d$ to be the i-th covariate vector and $y_i \in \mathbb{R}$ to be the i-th response in Equation (1). The tuple $(\boldsymbol{x}_i, y_i) \in \mathbb{R}^{d+1}$ is the i-th measurement. We study the problem under Gaussian design where each entry x_{ij}, for $i \in [n]$ and $j \in [d]$, is drawn i.i.d. from the standard normal distribution $\mathcal{N}(0, 1)$. Due to the quadratic nature of these measurements, the phase information is lost, making the recovery of the true signal $\boldsymbol{\theta}^* \in \mathbb{R}^d$ significantly challenging. Consequently, one can only hope to recover the signal up to a variation of its sign. Therefore, the output

---

[1]While the phase retrieval problem is also studied in the complex domain, we only focus on real signals in this work.

$\hat{\boldsymbol{\theta}}$ of any algorithm is measured (in the context of real signals) by evaluating $d(\hat{\boldsymbol{\theta}}, \boldsymbol{\theta}^*) \coloneqq \min\left\{\|\hat{\boldsymbol{\theta}} - \boldsymbol{\theta}^*\|, \|\hat{\boldsymbol{\theta}} + \boldsymbol{\theta}^*\|\right\}$. The difficulty is further compounded when some measurements can be *arbitrarily corrupted*. In this work, we aim to develop an algorithm for the phase retrieval problem that is robust to arbitrary corruption in k out of n measurements. To that end, we want to design and analyze algorithms to find $\hat{\boldsymbol{\theta}}$ and understand how $d(\hat{\boldsymbol{\theta}}, \boldsymbol{\theta}^*)$ depends on k and n. Below, we briefly outline the main contributions of this work:

- We propose an alternating minimization-based algorithm for phase retrieval with corrupted measurements. With only $n = \Omega\left(\frac{d\,\mathrm{polylog}(d)}{\epsilon^2 \log(\frac{1}{\epsilon})}\right)$ quadratic measurements and a corruption proportion of $\epsilon = \frac{k}{n}$, our algorithm achieves $d(\hat{\boldsymbol{\theta}}, \boldsymbol{\theta}^*) = \tilde{\mathcal{O}}\left(\sqrt{\epsilon}\right)$ with high probability, even under a strong corruption model (Bakshi and Prasad, 2021). To the best of our knowledge, this is the first algorithm for robust phase retrieval that provides an explicit expression for $d(\hat{\boldsymbol{\theta}}, \boldsymbol{\theta}^*)$ as a function of k and n. We also show that our algorithm stops in a finite number of iterations.

- Our high-probability guarantees are valid in regimes where $\epsilon\sqrt{\log \epsilon^{-1}} \log^2(\epsilon n) \to 0$ as $n \to \infty$. This includes the vanishing proportion regimes such as $k = n^{1-p}$ for $p \in (0, 1]$.

- In the first stage of our analysis, we assume the existence of an oracle capable of solving a nonconvex optimization problem to global optimality. In the second stage, we demonstrate that such an oracle can be efficiently constructed if the corruptions are independent of the covariates $\boldsymbol{x}_i$. This stage requires only $\mathcal{O}(d\,\mathrm{polylog}(d))$ quadratic measurements, ensuring that the overall sample complexity is not increased.

2 Solving The Phase Retrieval Problem

Considerable effort has been devoted to solving the phase retrieval problem in the uncorrupted setting (1). The work by Fienup (1982) surveys many classical methods for addressing phase retrieval. These methods often involve an alternating minimization approach (different from ours), which alternates between recovering signal information and phase information. However, these methods typically either provide only local optimal solutions or lack performance guarantees altogether. Recently, Netrapalli et al. (2013) proposed an alternating minimization approach and provided global convergence results using $\mathcal{O}(d\,\mathrm{polylog}(d))$ samples. Modern approaches to the phase retrieval problem can be broadly placed into two main categories.

2.0.1 Convex Formulations

Many approaches formulate the problem as a convex optimization problem, often using a semidefinite programming (SDP) formulation. They provide performance guarantees for signal recovery by solving their proposed convex relaxations (Candes et al., 2013; Candès and Li, 2014; Chen et al., 2015; Demanet and Hand, 2014; Waldspurger et al., 2015). While effective, these approaches suffer from heavy computational costs. Recently, new convex relaxations have been developed that work in the domain of the original variables, avoiding the high computational complexity associated with SDP relaxation (Goldstein and Studer, 2018; Bahmani and Romberg, 2017). These methods offer a more computationally efficient alternative while still providing provable performance guarantees.

2.0.2 Nonconvex Formulations

A more natural formulation of the signal recovery problem in phase retrieval leads to a nonconvex program:

$$\hat{\boldsymbol{\theta}} = \arg\min_{\boldsymbol{\theta} \in \mathbb{R}^d} \; f(\boldsymbol{\theta}) \coloneqq \frac{1}{4n} \sum_{i=1}^{n} \left(y_i - \langle \boldsymbol{x}_i, \boldsymbol{\theta} \rangle^2\right)^2. \tag{2}$$

Several methods have been proposed to solve this (or its nonsmooth variant) problem. Based on their initialization method, they can be further divided into two subcategories.

1. *Using spectral initialization:* The most notable approaches in this category utilize the Wirtinger flow algorithm or its variants (Candes et al., 2015; Chen and Candes, 2015; Zhang et al., 2016b; Wang et al., 2017). When initialized using a spectral method, they exhibit global convergence at a linear rate using only $\mathcal{O}(d\,\mathrm{polylog}(d))$ measurements. However, the spectral initialization requires an eigenvalue decomposition, which can be computationally expensive, involving costs comparable to matrix inversion.

2. *Using random initialization*: Sun et al. (2018) demonstrated that the nonconvex loss landscape of the phase retrieval problem (2) possesses special geometric properties. They proved that with $\mathcal{O}(d\log^3 d)$ measurements, all the local minima of the loss function are also global minima, and all the saddle points are strict

saddle points (Ge et al., 2015). This property allows any saddle point-escaping algorithms, such as Hessian-based methods (Nesterov and Polyak, 2006; Sun et al., 2018), perturbed gradient descent (Jin et al., 2017), stochastic-gradient descent (Ge et al., 2015), and normalized gradient descent (Murray et al., 2017), to converge to the global minima of the phase retrieval problem (2) without requiring spectral initialization. However, these methods often incur high iteration complexity, typically at least $\mathcal{O}(d^{2.5})$. Notable exceptions include the work by Tan and Vershynin (2023), which requires only $\mathcal{O}(d \operatorname{polylog}(d))$ iterations with stochastic gradient updates (on the nonsmooth variant), and the work by Chen et al. (2019), which needs only $\mathcal{O}(\log d)$ iterations with full gradient updates.

3 Phase Retrieval With Corruptions

The primary applications of phase retrieval (Walther, 1963; Millane, 1990) are susceptible to corrupted measurements due to instrument failures, Byzantine sensors, or other measurement errors (Weller et al., 2015). Therefore, the data generation model in (1) can be modified to account for these corruptions as follows:

$$y_i = \langle \boldsymbol{x}_i, \boldsymbol{\theta}^* \rangle^2 + \eta_i, \quad i \in [n] \,, \tag{3}$$

where corruption in i-th measurement is denoted as $\eta_i \in \mathbb{R}$ and drawn from an unknown distribution $\mathcal{P}_\eta$. We collect all the η_i's in a vector $\boldsymbol{\eta} \in \mathbb{R}^n$. Furthermore, we assume $\|\boldsymbol{\eta}\|_0 = k$. The set $C^* := \big\{ i \in [n] \,|\, \eta_i \neq 0 \big\}$ contains the indices of corrupted measurements. The task still remains to learn $\boldsymbol{\theta}^*$ from the quadratic measurements of the form $(\boldsymbol{x}_i, y_i), \forall i \in [n]$. We allow an adversary to arbitrarily corrupt $\epsilon = \frac{k}{n}$ fraction of responses, where $k = k_n$ is allowed to grow with n. We adopt a *strong corruption model* (Bakshi and Prasad, 2021) in our setting. Before introducing corruption, the adversary has full information about the measurements and the estimator.

Definition 1 (Strong Corruption Model). *In this corruption model, the data generation process involves two steps:*

1. *Clean measurements $(\boldsymbol{x}_i, y_i), i \in [n]$ are generated according to the noiseless data generation model given by* (1). *These measurements are collected in a set S.*

2. *The adversary selects any subset $C^* \subseteq [n]$ of size k. For each $i \in C^*$, the adversary replaces y_i with $y_i + \eta_i$, where η_i is drawn from an unknown distribution $\mathcal{P}_\eta$. Notably, the adversary can choose η_i that depends on the measurements $(\boldsymbol{x}_i, y_i)$.*

This corruption model stands as the most stringent, encompassing a wide array of other response corruption models, including the Huber contamination model and sparse arbitrary outliers model (Huang et al., 2023). We note that a strong adversary could consistently set an ϵ proportion of measurements to be identical, even if those measurements originate from two distinct distributions following (3). These distributions could differ by at most $1 - \epsilon$ in terms of total variation distance. Consequently, a high probability exact recovery guarantee becomes unattainable when ϵ is constant.

(a) No corruption

(b) Average corruption $\bar{\eta} \leq -3\|\boldsymbol{\theta}^*\|^2$

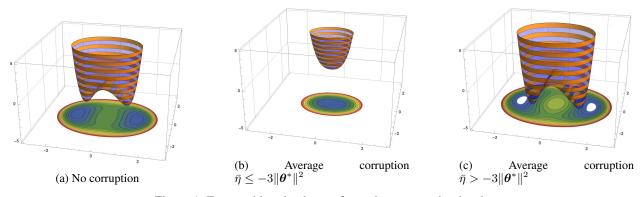(c) Average corruption $\bar{\eta} > -3\|\boldsymbol{\theta}^*\|^2$

Figure 1: Expected loss landscape for various corruption levels

Proposition 1 (Impossibility with constant corruption proportion). *If the measurements follow the data generation process* (3) *with a corruption proportion $\epsilon > 0$, then for any estimator $\hat{\boldsymbol{\theta}}$ and any $\delta > 0$:*

$$\mathbb{P}\big[d(\hat{\boldsymbol{\theta}}, \boldsymbol{\theta}^*) \geq \delta\big] \geq \frac{\epsilon}{2} \,.$$

Under the strong corruption model, Proposition 1 states that estimation of $\boldsymbol{\theta}^*$ (up to its sign) fails with a constant probability when ϵ is a constant. Therefore, this work concentrates on the scenarios where the corruption proportion vanishes with n, i.e., $\epsilon = \epsilon_n \to 0$ as $n \to \infty$.

Efforts have been made to extend phase retrieval algorithms to settings involving corrupted measurements. Hand (2017) showed that PhaseLift (Candes et al., 2013) is robust to a sufficiently small proportion of corrupted measurements, although the explicit proportion of corruption it can handle is not provided. Recently, Huang et al. (2023) proposed a convex relaxation-based approach capable of handling approximately 11.85% of corrupted measurements. They also demonstrated that this bound cannot be improved for their method. These approaches are computationally expensive due to their reliance on SDP relaxation. In contrast, Zhang et al. (2016a) proposed a computationally efficient approach using truncated Wirtinger flow, which can handle a small number of corrupted measurements with only $\mathcal{O}(d\operatorname{polylog}(d))$ samples and $\mathcal{O}(d^2\operatorname{polylog}(d))$ iteration complexity. Existing works (Hand, 2017; Huang et al., 2023; Zhang et al., 2016b) in robust phase retrieval provide convergence guarantees for the estimator $\hat{\boldsymbol{\theta}}$ of the true parameter $\boldsymbol{\theta}^*$. However, these works do not explicitly address the dependency of convergence on the number of corrupted measurements k relative to the total number of measurements n. Consequently, predicting the impact of an increasing proportion of corruption on the convergence rate remains difficult. This leads to the following critical problem of interest:

Problem 1 (Robust Phase Retrieval). *Can we propose a sample and computationally efficient algorithm that outputs an estimate $\hat{\boldsymbol{\theta}}$ of the true parameter $\boldsymbol{\theta}^*$ that allows us to identify a function $g(k,n)$ such that*

$$d(\hat{\boldsymbol{\theta}}, \boldsymbol{\theta}^*) \le g(k,n) \, ,$$

and characterize regimes of $\epsilon = \epsilon_n = k/n$ such that $g(k,n) \to 0$ as $n \to \infty$?

We provide an affirmative answer to Problem 1 by proposing an efficient alternating minimization-based algorithm.

4   Alternating Minimization Algorithm

The main intuition behind the alternating minimization approach stems from a couple of key observations.

4.1   Geometry of the loss function

Our first observation pertains to the geometrical properties of the objective function in the optimization problem (2). Although the optimization problem (2) is nonconvex, it can be analyzed due to the favorable geometric properties of its objective function (Sun et al., 2018). Indeed, numerous methods (Ge et al., 2015; Nesterov and Polyak, 2006; Sun et al., 2018; Jin et al., 2017; Ge et al., 2015; Murray et al., 2017) discussed in Section 2 leverage this benign geometry to develop efficient algorithms with provable guarantees for solving (2). If the corrupted measurements do not significantly distort this geometry, we can still apply the methods outlined in Section 2 to handle the corruption. To illustrate, consider Figure 1 where the expected objective function for problem (2), defined as $F(\boldsymbol{\theta}, \boldsymbol{\eta}) := \mathbb{E}_{\boldsymbol{x}_1, \ldots, \boldsymbol{x}_n}\big[f(\boldsymbol{\theta})\big]$, is graphically visualized for a two-dimensional example. When the corruptions η_i are independently chosen from $\boldsymbol{x}_i$, the shape of the loss function is influenced by the average corruption $\bar{\eta} = \frac{1}{n}\sum_{i=1}^{n}\eta_i$. Specifically, the function maintains a similar shape as the uncorrupted case when $\bar{\eta} > -3\|\boldsymbol{\theta}^*\|^2$, and becomes convex when $\bar{\eta} \le -3\|\boldsymbol{\theta}^*\|^2$. These insights suggest that (2) can be solved even with corrupted measurements. Therefore, we introduce the LSQ-PHASE-ORACLE (Algorithm 1), an oracle algorithm designed to solve the least squares formulation of the phase retrieval problem even when faced with corrupted measurements. Under mild assumptions regarding corruption, several methods described in Section 2 can be utilized for this purpose. We provide an efficient construction of one such oracle in Section 7.

Algorithm 1 LSQ-PHASE-ORACLE

Input: $U \subseteq [n], S = \{(\boldsymbol{x}_1, y_1), \ldots, (\boldsymbol{x}_n, y_n)\}$
Output: $\tilde{\boldsymbol{\theta}}$

1: $\tilde{\boldsymbol{\theta}} = \arg\min_{\boldsymbol{\theta} \in \mathbb{R}^d} \frac{1}{4|U|} \sum_{i \in U} \left(y_i - \langle \boldsymbol{x}_i, \boldsymbol{\theta}\rangle^2\right)^2.$
2: **return** $\tilde{\boldsymbol{\theta}}$.

4.2 Filtering the corrupted measurements

Our second observation provides a counterbalance to our first observation. Despite the favorable geometric properties of the objective function, one cannot hope to reconstruct the true signal $\boldsymbol{\theta}^*$ by directly solving the nonconvex optimization problem (2) in the presence of corrupted measurements. If we had prior knowledge of which measurements were uncorrupted, we could solve problem (2) using only those uncorrupted measurements. However, in the absence of such information, we must reformulate it into another, potentially more challenging, nonconvex problem. To reduce the impact of obviously corrupted measurements, we initially preprocess the data by discarding measurements with negative y_i's. We further trim the dataset by eliminating measurements with the largest y_i values, ensuring the remaining set consists of $n - k$ measurements. This refined set of measurements is denoted by $\tilde{S} \subset [n]$ with $|\tilde{S}| = n - k$. It is important to note that even after preprocessing step, $\tilde{S}$ might still contain up to k corrupted measurements, although their values are restricted from being excessively large. We construct the following optimization problem after preprocessing:

$$\left(\hat{\boldsymbol{\theta}}, \hat{U}\right) = \underset{\boldsymbol{\theta} \in \mathbb{R}^d, U}{\arg\min} \, f(U, \boldsymbol{\theta}) \coloneqq \frac{1}{4|U|} \sum_{i \in U} \left(y_i - \langle \boldsymbol{x}_i, \boldsymbol{\theta} \rangle^2 \right)^2$$

$$\text{such that } U \subset \tilde{S}, \ |U| = n - 2k \tag{4}$$

Ideally, we want to select $n - 2k$ uncorrupted samples from $\tilde{S}$ and use them to estimate $\boldsymbol{\theta}^*$; this explains the term $n - 2k$ in (4). A natural approach of solving problem (4) is to use an alternating minimization strategy. This method iterates between two steps: first, solving for $\boldsymbol{\theta}$ with a fixed U, and then updating U based on the obtained $\boldsymbol{\theta}$. We formally present this approach as ALT-MIN-PHASE in Algorithm 2.

Algorithm 2 ALT-MIN-PHASE

Input: $S = \{(\boldsymbol{x}_1, y_1), \ldots, (\boldsymbol{x}_n, y_n)\}$
Parameters: $k, \ \beta > 0$
Output: $\hat{\boldsymbol{\theta}}$ – An estimate of $\boldsymbol{\theta}^*$
 1: $\boldsymbol{\theta}^1 = \mathbf{0} \in \mathbb{R}^d$.
 2: **Preprocessing:**
 3: Discard measurements with negative y_i's
 4: From the remaining measurements discard measurements with the largest y_i to construct $\tilde{S}$ with $|\tilde{S}| = n - k$
 5: **for** $t = 1, 2 \ldots$ **do**
 6: $\quad U^t = \arg\min_{U \subset \tilde{S}, |U| = n - 2k} \sum_{i \in U} f_i(\boldsymbol{\theta}^t),$
     $\quad$ where $f_i(\boldsymbol{\theta}) = \left(y_i - \langle \boldsymbol{x}_i, \boldsymbol{\theta} \rangle^2 \right)^2$
 7: $\quad \boldsymbol{\theta}^{t+1} = \text{LSQ-PHASE-ORACLE}(U^t).$
 8: $\quad$ **if** $\frac{1}{4|U^t|} \sum_{i \in U^t} \left(f_i(\boldsymbol{\theta}^t) - f_i(\boldsymbol{\theta}^{t+1}) \right) < \beta$ **then**
 9: $\quad\quad \hat{U} = U^t, \ \hat{\boldsymbol{\theta}} = \boldsymbol{\theta}^t.$
10: $\quad\quad$ STOP.
11: $\quad$ **end if**
12: **end for**
13: **return** $\hat{\boldsymbol{\theta}}$.

Leveraging tail bounds of maximum of the chi-squared random variables, the preprocessing step effectively removes the measurements i for which $\eta_i = \Omega(\log n)$ with high probability. Following this, the algorithm employs an alternating minimization strategy on the remaining measurements, utilizing LSQ-PHASE-ORACLE as a subroutine to solve (2) with corruption. The process continues until the decrease of the objective function value is less than a certain predefined threshold $\beta > 0$ (to be fixed later). Intuitively, ALT-MIN-PHASE aims to produce a set $\hat{U}$ that contains indices of either uncorrupted measurements or corrupted measurements with minimal corruption. The key idea is that using such a $\hat{U}$ as input to the LSQ-PHASE-ORACLE will provide a good estimate of $\boldsymbol{\theta}^*$. However, this guarantee is not obvious. Given the nonconvex nature of problem (4), ALT-MIN-PHASE is likely to converge to a stationary point. Therefore, before presenting the theoretical guarantees for our approach, we demonstrate its practical efficacy through numerical experiments.

4.3 Numerical Experiments

We evaluated the practicality of our approach through numerical experiments with varying degrees of corruption. We analyzed the effect of increasing the number of measurements on the relative error, defined as $\frac{d(\hat{\boldsymbol{\theta}}, \boldsymbol{\theta}^*)}{\|\boldsymbol{\theta}^*\|}$. The corruption
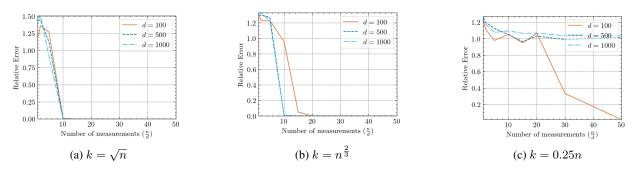
Figure 2: Performance of ALT-MIN-PHASE (Algorithm 2) with varying degrees of corrupted measurements.

values η_i were drawn uniformly at random from $[-5, 5]$. We used gradient descent with random initialization (Chen et al., 2019) as the oracle algorithm. Figure 2 presents the results of our experiments for three different corruption proportions, $\frac{k}{n} \in \{\frac{1}{\sqrt{n}}, \frac{1}{n^{1/3}}, 0.25\}$. The plots correspond to $d \in \{100, 500, 1000\}$. We make the following observations:

1. For $k \in \{\sqrt{n}, n^{\frac{2}{3}}\}$ (i.e., $\epsilon = o(1)$), Figures 2a and 2b demonstrate that the alternating minimization approach accurately recovers $\boldsymbol{\theta}^*$ for each $d \in \{100, 500, 1000\}$.

2. The proposed approach does not always yield a good estimate of $\boldsymbol{\theta}^*$ when there is a constant proportion of corruptions which is expected from Proposition 1.

Next, we present our theoretical results that explain these empirical observations.

5   Main Theoretical Result

In this section, we present a theoretical analysis of ALT-MIN-PHASE. While alternating minimization algorithms are known to converge to a stationary point for nonconvex problems, the resulting solution may not be close to the global minimum. Our analysis aims to characterize the properties of the converged stationary point and demonstrate its proximity to the global minimum. Although our problem and setting are entirely different, our analysis follows a framework similar to Chen et al. (2022), which addresses fixed-design linear regression with Huber corruption. The quartic nature of the objective function in (4) imposes strong constraints on the handling of the spectral properties of the Hessian of the loss function, as well as on the concentration and tail bounds involved in the analysis. One immediate consequence of these constraints is the limited regime of corruption proportions that can be effectively managed by Algorithm 2 with $n = \mathcal{O}(d \operatorname{polylog}(d))$ measurements. We begin by characterizing this restricted regime. For a proportion of corruption ϵ, we define

$$\Delta(k, n) := \epsilon \sqrt{\log \epsilon^{-1}} \log^2(\epsilon n).$$

For brevity, we sometimes use Δ to denote $\Delta(k, n)$. We define the *favorable corruption* regime $\mathcal{K}$ as the set of all increasing sequences $\{k_n\}_{n=1}^\infty$ satisfying

$$\mathcal{K} := \left\{ \{k_n\}_{n=1}^\infty \subseteq \mathbb{N} \mid \lim_{n \to \infty} \Delta(k_n, n) = 0, \ \frac{k_n}{n} < \frac{1}{2} \right\}.$$

We remark that $\mathcal{K}$ captures all corruption regimes such that $k = \mathcal{O}(n^{1-p})$ with $p \in (0, 1]$. On the other hand, it does not contain constant corruption proportion regimes in which $k = \Theta(n)$. With this understanding, we are ready to state the main convergence guarantees for Algorithm 2.

Theorem 1. *Let $S = \{(\boldsymbol{x}_i, y_i)\}_{i=1}^n$ be a set of measurements generated by the strong corruption model with corruption proportion $\epsilon = \frac{k}{n}$. We further assume that $k \in \mathcal{K}$. Let $n = \Omega\left(\frac{d \operatorname{polylog}(d) + \log(\frac{1}{\delta})}{\epsilon^2 \log(\frac{1}{\epsilon})}\right)$ for some $\delta \in (0, 1]$. With probability at least $1 - \delta - \mathcal{O}(\frac{1}{n})$, Algorithm 2 with parameters k and $\beta = \epsilon^2$ terminates within $\mathcal{O}(\frac{\sum_{i=1}^n y_i^2}{4(n-k)\epsilon^2})$ iterations, and outputs an estimate $\hat{\boldsymbol{\theta}}$ such that for some absolute constants $C_1, C_2, C_3 > 0$*

$$d(\hat{\boldsymbol{\theta}}, \boldsymbol{\theta}^*) \le 1.2 \max \left\{ \left(\psi(k, n, \boldsymbol{\eta})\right)^{\frac{1}{2}}, \psi(k, n, \boldsymbol{\eta}) \right\} \sqrt{\epsilon},$$

where $\psi(k, n, \boldsymbol{\eta}) = \frac{\sqrt{(C_1 + \max_i |\eta_i|)(1 + \Delta)}}{(1 - 3\epsilon)(C_2 - \Delta) - C_3 \Delta}$.

Before we present a proof sketch, several remarks are in order to understand Theorem 1:

1. It may appear that $\psi(k, n, \boldsymbol{\eta})$ can grow rapidly if the amount of corruption $\max_i |\eta_i|$ is large. However, it should be remembered that due to the preprocessing step performed by Algorithm 2, the growth of $\max_i |\eta_i|$ is not fast. In fact, it can be shown that its value is upper bounded by $\mathcal{O}(\log n)$ with high probability. Since $\psi(k, n, \boldsymbol{\eta}) = \mathcal{O}(\sqrt{\log n})$, the convergence rate of the Algorithm 2 is primarily determined by $\sqrt{\epsilon}$.

2. The dependence of n on ϵ might initially seem counterintuitive, but it aligns with standard results in robust statistics (Chen et al., 2022; Gao, 2020; Diakonikolas et al., 2019). In practice, one can typically assume ϵ to be bounded away from zero by artificially considering some of the uncorrupted measurements as corrupted.

3. The theoretical analysis of ALT-MIN-PHASE can be extended to phase retrieval with additive Gaussian noise, i.e., the uncorrupted measurements are $y_i + e_i$ where e_i is an independent additive Gaussian noise. The fundamental analysis still applies, with the added consideration of concentration inequalities involving the noise variance.

In the following section, we offer a proof sketch highlighting the key elements of the proof for Theorem 1 when $k \in \mathcal{K}$. Due to space limitations, the complete proof is provided in Appendix A.

6 Proof Sketch of Theorem 1

For a fixed set $U \subseteq [n]$, we define the loss function $f_U(\boldsymbol{\theta})$ along with its gradient $\nabla f_U(\boldsymbol{\theta})$ as follows:

$$f_U(\boldsymbol{\theta}) = \frac{1}{4|U|} \sum_{i \in U} \left(\langle \boldsymbol{x}_i, \boldsymbol{\theta} \rangle^2 - y_i \right)^2$$

$$\nabla f_U(\boldsymbol{\theta}) = \frac{1}{|U|} \sum_{i \in U} \left(\langle \boldsymbol{x}_i, \boldsymbol{\theta} \rangle^2 - y_i \right) \boldsymbol{x}_i \boldsymbol{x}_i^\top \boldsymbol{\theta}$$

Our analysis of ALT-MIN-PHASE is conducted in two stages. First, we demonstrate that the output $\hat{\boldsymbol{\theta}}$ from Algorithm 2 is indeed a γ-approximate stationary point of $f_{\hat{U}}(\boldsymbol{\theta})$ which is defined as:

$$\langle \nabla f_{\hat{U}}(\hat{\boldsymbol{\theta}}), \hat{\boldsymbol{\theta}} - \boldsymbol{\theta}^* \rangle \leq \gamma \|\hat{\boldsymbol{\theta}} - \boldsymbol{\theta}^*\| .$$

After that, we establish that this approximate stationary point is close to the true signal $\boldsymbol{\theta}^*$ in terms of $d(\hat{\boldsymbol{\theta}}, \boldsymbol{\theta}^*)$.

6.1 Convergence to An Approximate Stationary Point

We begin by showing that the output of Algorithm 2 is an approximate stationary point. Before we present the formal statement, we define the following quantity for some absolute constants C_1, C_2 and $C_3 > 0$:

$$L(\hat{\boldsymbol{\theta}}, \boldsymbol{\theta}^*, \Delta, \boldsymbol{\eta}) \coloneqq \frac{1}{2}\left((C_1 + \Delta)\|\hat{\boldsymbol{\theta}} - \boldsymbol{\theta}^*\|^2 + (C_2 + \Delta)\|\hat{\boldsymbol{\theta}} - \boldsymbol{\theta}^*\| + (C_3 + \Delta) + \max_{i \in U} |\eta_i|\big(1 + \Delta\big) \right).$$

The following lemma shows that if we set $\gamma = 2\sqrt{L(\hat{\boldsymbol{\theta}}, \boldsymbol{\theta}^*, \Delta, \boldsymbol{\eta})}\epsilon$, the output of Algorithm 2 is an γ-approximate point of $f_{\hat{U}}(\boldsymbol{\theta})$.

Lemma 1. *If* $n = \Omega\big(\frac{d\,\mathrm{polylog}(d) + \log(\frac{1}{\delta})}{\epsilon^2 \log(\frac{1}{\epsilon})}\big)$, *then the output* $\hat{\boldsymbol{\theta}}$ *Algorithm 2 is a* $2\sqrt{L(\hat{\boldsymbol{\theta}}, \boldsymbol{\theta}^*, \Delta, \boldsymbol{\eta})}\epsilon$-*stationary point of* $f_{\hat{U}}(\boldsymbol{\theta})$ *with probability at least* $1 - \delta - \mathcal{O}(\frac{1}{n})$.

The convergence of the Algorithm 2 depends on the spectral properties of $\nabla^2 f_{\hat{U}}(\boldsymbol{\theta})$. Specifically, one can employ the descent lemma to study the convergence properties of the Algorithm 2 if the spectral norm of $\nabla^2 f_{\hat{U}}(\boldsymbol{\theta})$ is uniformly upper bounded by a constant for all $\boldsymbol{\theta} \in \mathbb{R}^d$. Unfortunately, due to the quartic nature of $f_{\hat{U}}(\boldsymbol{\theta})$, this property does not hold in general. To overcome this challenge, we study the spectral properties of $\nabla^2 f_{\hat{U}}(\boldsymbol{\theta})$ for $\boldsymbol{\theta}$ belonging to a specific set relevant to our setting. This leads to the following lemma.

Lemma 2. *If* $\boldsymbol{\theta}$ *lies on the line segment connecting* $\hat{\boldsymbol{\theta}}$ *and* $\boldsymbol{\theta}^*$ *and* $n = \Omega\big(\frac{d\,\mathrm{polylog}(d) + \log(\frac{1}{\delta})}{\epsilon^2 \log(\frac{1}{\epsilon})}\big)$ *for some* $\delta \in (0, 1]$, *then with probability at least* $1 - \delta - \mathcal{O}(\frac{1}{n})$,

$$(\hat{\boldsymbol{\theta}} - \boldsymbol{\theta}^*)^\top \nabla^2 f_{\hat{U}}(\boldsymbol{\theta})(\hat{\boldsymbol{\theta}} - \boldsymbol{\theta}^*) \leq 2L(\hat{\boldsymbol{\theta}}, \boldsymbol{\theta}^*, \Delta, \boldsymbol{\eta})\|\hat{\boldsymbol{\theta}} - \boldsymbol{\theta}^*\|^2.$$

With Lemma 2 in place, a modified version of the descent lemma follows immediately.

Lemma 3. *Let $\bar{\theta}$ be any point on the line segment connecting $\hat{\theta}$ and θ^*. Assume that the following properties hold:*

1. $\langle \nabla f_{\hat{U}}(\hat{\theta}), \hat{\theta} - \theta^* \rangle \geq \gamma \|\hat{\theta} - \theta^*\| > 0$ *and*

2. $\frac{\hat{\theta} - \theta^*}{\|\hat{\theta} - \theta^*\|} \nabla^2 f_{\hat{U}}(\bar{\theta}) \frac{\hat{\theta} - \theta^*}{\|\hat{\theta} - \theta^*\|} \leq 2L(\hat{\theta}, \theta^*, \Delta, \boldsymbol{\eta}).$

Then, there exists $\boldsymbol{\theta} \in \mathbb{R}^d$ such that

$$f_{\hat{U}}(\boldsymbol{\theta}) \leq f_{\hat{U}}(\hat{\theta}) - \frac{\gamma^2}{4L(\hat{\theta}, \theta^*, \Delta, \boldsymbol{\eta})} \; .$$

If the Algorithm 2 stops, then it means that the decrease in the objective function is less than β. By the contrapositive, it implies that $\beta \geq \frac{\gamma^2}{4L(\hat{\theta}, \theta^*, \Delta, \boldsymbol{\eta})}$ and

$$\langle \nabla f_{\hat{U}}(\hat{\theta}), \hat{\theta} - \theta^* \rangle \leq 2\sqrt{L(\hat{\theta}, \theta^*, \Delta, \boldsymbol{\eta})\beta} \|\hat{\theta} - \theta^*\| \; .$$

Picking $\beta = \epsilon^2$ proves Lemma 1. Observe that Algorithm 2 must terminate in a finite number of steps. For $\boldsymbol{\theta} = \mathbf{0}$, initial value of $f_U(\boldsymbol{\theta})$ is not more than $\frac{\sum_{i=1}^n y_i^2}{4(n-2k)}$, and it decreases by at least $\beta > 0$ at each iteration. Since the objective function cannot assume negative values, the algorithm must terminate after at most $\frac{\sum_{i=1}^n y_i^2}{4(n-2k)\epsilon^2}$ iterations.

6.2 Proximity to the Ground Truth

In this subsection, we build on the results from Lemma 1 to show that $\hat{\theta}$ is close to θ^*. First, observe that $d(\boldsymbol{\theta}, \theta^*)$ can be treated as $\|\boldsymbol{\theta} - \theta^*\|$ without loss of generality by possibly flipping the sign of θ^*. By setting $\gamma = 2\sqrt{L(\hat{\theta}, \theta^*, \Delta, \boldsymbol{\eta})}\epsilon$, we can express the results from Lemma 1 as follows:

$$\frac{1}{|\hat{U}|} \sum_{i \in \hat{U}} \Big(\langle \boldsymbol{x}_i, \hat{\theta} \rangle^2 - y_i \Big) \boldsymbol{x}_i^\top \hat{\theta} \big(\hat{\theta} - \theta^* \big)^\top \boldsymbol{x}_i \leq \gamma \|\hat{\theta} - \theta^*\| \; .$$

Recall that $|\hat{U}| < n$ and it contains both corrupted and uncorrupted measurements. Specifically, the measurements in $\hat{U}$ can be partitioned into two disjoint sets $\hat{U} \cap U^*$ and $\hat{U} \cap C^*$ where C^* is defined in Definition 1 and $U^* = [n] \setminus C^*$. Given these observations, we can rearrange terms to get:

$$\underbrace{\frac{1}{n} \sum_{i \in \hat{U} \cap U^*} \Big(\langle \boldsymbol{x}_i, \hat{\theta} \rangle^2 - y_i \Big) \boldsymbol{x}_i^\top \hat{\theta} \big(\hat{\theta} - \theta^* \big)^\top \boldsymbol{x}_i}_{\zeta(\hat{\theta}, \theta^*, n, k)} \leq \gamma \|\hat{\theta} - \theta^*\| - \underbrace{\frac{1}{n} \sum_{i \in \hat{U} \cap C^*} \Big(\langle \boldsymbol{x}_i, \hat{\theta} \rangle^2 - y_i \Big) \boldsymbol{x}_i^\top \hat{\theta} \big(\hat{\theta} - \theta^* \big)^\top \boldsymbol{x}_i}_{\xi(\hat{\theta}, \theta^*, n, k, \boldsymbol{\eta})}$$

Our aim is to provide a lower bound on $\zeta(\hat{\theta}, \theta^*, n, k)$ and an upper bound on $\xi(\hat{\theta}, \theta^*, n, k, \boldsymbol{\eta})$, both in terms of $\|\hat{\theta} - \theta^*\|$. Note that $\zeta(\hat{\theta}, \theta^*, n, k)$ does not contain any corrupted measurements. Therefore, we can simply replace y_i with $\langle \boldsymbol{x}_i, \theta^* \rangle^2$ using the data generation process in (1). The following lemma provides a lower bound on $\zeta(\hat{\theta}, \theta^*, n, k)$.

Lemma 4. *If $n = \Omega\big(\frac{d \operatorname{polylog}(d) + \log(\frac{1}{\delta})}{\epsilon^2 \log(\frac{1}{\epsilon})} \big)$ for some $\delta \in (0, 1]$, then for some absolute constants C_1, C_2 and $C_3 > 0$, the following holds with probability at least $1 - \delta - \mathcal{O}(\frac{1}{n})$:*

$$\zeta(\hat{\theta}, \theta^*, n, k) \geq (1 - 3\epsilon)\Big(\big(C_1 - \Delta\big)\|\hat{\theta} - \theta^*\|^4 + \big(C_2 - \Delta\big)\|\hat{\theta} - \theta^*\|^3 + \big(C_3 - \Delta\big)\|\hat{\theta} - \theta^*\|^2 \Big) \; .$$

Extra care is needed to handle $\xi(\hat{\theta}, \theta^*, n, k, \boldsymbol{\eta})$ as it involves corrupted measurements. Using the Cauchy-Schwartz inequality,

$$\xi(\hat{\theta}, \theta^*, n, k, \boldsymbol{\eta}) \leq \underbrace{\Big(\frac{1}{n} \sum_{i \in \hat{U} \cap C^*} \big(\langle \boldsymbol{x}_i, \hat{\theta} \rangle^2 - y_i \big)^2 \Big)^{\frac{1}{2}}}_{\xi_1(\hat{\theta}, \theta^*, n, k, \boldsymbol{\eta})} \times \underbrace{\Big(\frac{1}{n} \sum_{i \in \hat{U} \cap C^*} \big(\boldsymbol{x}_i^\top \hat{\theta} \big(\hat{\theta} - \theta^* \big)^\top \boldsymbol{x}_i \big)^2 \Big)^{\frac{1}{2}}}_{\xi_2(\hat{\theta}, \theta^*, n, k)} \; .$$

For a fixed $\hat{\boldsymbol{\theta}}$, Algorithm 2 outputs $\hat{U}$ that yields the smallest loss. By removing the measurements belonging to $\hat{U} \cap U^*$ from both $\hat{U}$ and U^*, we obtain

$$\xi_1(\hat{\boldsymbol{\theta}}, \boldsymbol{\theta}^*, n, k, \boldsymbol{\eta}) \le \frac{1}{n} \sum_{i \in U^* \setminus \hat{U}} \left(\langle \boldsymbol{x}_i, \hat{\boldsymbol{\theta}} \rangle^2 - y_i \right)^2. \tag{5}$$

Note that the right-hand side of (5) contains terms that represent uncorrupted measurements. This allows us to provide an upper bound on $\xi_1(\hat{\boldsymbol{\theta}}, \boldsymbol{\theta}^*, n, k, \boldsymbol{\eta})$ that is independent of $\boldsymbol{\eta}$. Similarly, $\xi_2(\hat{\boldsymbol{\theta}}, \boldsymbol{\theta}^*, n, k)$ does not involve any y_i and thus remains unaffected by the corrupted measurements. We provide an upper bound on both terms in the following lemma.

Lemma 5. *Let* $n = \Omega\left(\frac{d \operatorname{polylog}(d) + \log(\frac{1}{\delta})}{\epsilon^2 \log(\frac{1}{\epsilon})}\right)$ *for some* $\delta \in (0, 1]$ *and for some absolute constants* C_1, C_2 *and* $C_3 > 0$, *define*

$$\upsilon(\hat{\boldsymbol{\theta}}, \boldsymbol{\theta}^*, n, k) \coloneqq C_1 \Delta \|\hat{\boldsymbol{\theta}} - \boldsymbol{\theta}^*\|^4 + C_2 \Delta \|\hat{\boldsymbol{\theta}} - \boldsymbol{\theta}^*\|^3 + C_3 \Delta \|\hat{\boldsymbol{\theta}} - \boldsymbol{\theta}^*\|^2 \,.$$

Then, with probability at least $1 - \delta - \mathcal{O}(\frac{1}{n})$:

1. $\xi_1(\hat{\boldsymbol{\theta}}, \boldsymbol{\theta}^*, n, k, \boldsymbol{\eta}) \le \upsilon(\hat{\boldsymbol{\theta}}, \boldsymbol{\theta}^*, n, k)$

2. $\xi_2(\hat{\boldsymbol{\theta}}, \boldsymbol{\theta}^*, n, k) \le \upsilon(\hat{\boldsymbol{\theta}}, \boldsymbol{\theta}^*, n, k)$

3. *Consequently,* $\xi(\hat{\boldsymbol{\theta}}, \boldsymbol{\theta}^*, n, k, \boldsymbol{\eta}) \le \upsilon(\hat{\boldsymbol{\theta}}, \boldsymbol{\theta}^*, n, k)$.

Now we substitute $\gamma = 2\sqrt{L(\hat{\boldsymbol{\theta}}, \boldsymbol{\theta}^*, \Delta, \boldsymbol{\eta})}\epsilon$ and combine Lemmas 4 and 5 which finally leads to Theorem 1.

7 Constructing LSQ-PHASE-ORACLE

Our theoretical results so far assume the existence of an oracle in Algorithm 1. Note that the optimization problem addressed by the LSQ-PHASE-ORACLE is inherently nonconvex, even in the absence of corruption. However, in the absence of corruption, this problem can be efficiently solved due to its "benign" loss landscape. When arbitrary corruption is introduced under the strong corruption model, this benign geometry may not be preserved. To address this, we introduce an additional assumption in our corruption model to maintain the favorable geometric properties necessary for efficient optimization, at least with high probability.

Assumption 1. *For each* $i \in C^*$, *the adversary draws* $\eta_i \sim \mathcal{P}_\eta$ *independently of* $\boldsymbol{x}_i$.

The corruption model under Assumption 1 is also known as the sparse arbitrary outliers model (Huang et al., 2023). Figure 1 illustrates the loss landscape of (4) under Assumption 1 for various levels of corruption. The solution provided by LSQ-PHASE-ORACLE, when used in isolation, can be far from the ground truth $\boldsymbol{\theta}^*$. Therefore, to filter out the corrupted measurements, an alternating minimization procedure is necessary even with an oracle. While many approaches mentioned in Section 2 can be extended to work for our setting, we opt to use the gradient descent approach with random initialization (Chen et al., 2019) as the oracle.

7.1 Random Initialized Gradient Descent For Corrupted Measurements

Chen et al. (2019) demonstrated that by analyzing the dynamics of the approximate state evolution of fixed step gradient descent updates, it is possible to show that randomly initialized gradient descent algorithm with a fixed step size converges linearly to the true solution, $\boldsymbol{\theta}^*$, in the uncorrupted case. They carefully use a leave-one-out approach to handle the dependence between $\boldsymbol{x}_i$ and the iterates. We argue that their method can also be extended to the corrupted case under Assumption 1. We employ a modified version of their leave-one-out approach, with an adjusted initialization, and extend their results by examining various corruption scenarios separately. We present a modified version of Chen et al. (2019)'s algorithm in Algorithm 3. Under Assumption 1, the geometry of the loss in equation (2) is influenced by the average corruption, defined as $\bar{\eta} = \frac{1}{n} \sum_{i=1}^{n} \eta_i$. Analyzing the loss $F(\boldsymbol{\theta}, \boldsymbol{\eta})$, we observe that when $\bar{\eta} > -3\|\boldsymbol{\theta}^*\|^2$, the loss landscape maintains a similar geometry to the no-corruption case but with a displaced global minimum occurring at $\pm\kappa\boldsymbol{\theta}^*$ where $\kappa \coloneqq \sqrt{1 + \frac{\bar{\eta}}{3\|\boldsymbol{\theta}^*\|^2}}$. Conversely, when $\bar{\eta} \le -3\|\boldsymbol{\theta}^*\|^2$, the loss becomes convex with its minimum occurring at $\mathbf{0} \in \mathbb{R}^d$. Algorithm 3 computes κ_{sq} which, in expectation, is equal to κ^2. A negative value of κ_{sq} indicates that $\bar{\eta} \le -3\|\boldsymbol{\theta}^*\|^2$. Therefore, Algorithm 3 returns $\mathbf{0}$ in this scenario. In the alternative case where $\bar{\eta} > -3\|\boldsymbol{\theta}^*\|^2$, we present the following convergence result:

Algorithm 3 GRADIENT DESCENT WITH RANDOM INIT

Input: $U \subseteq [n], S = \{(\boldsymbol{x}_1, y_1), \ldots, (\boldsymbol{x}_n, y_n)\}$
Parameters: $\mu = \frac{c}{\|\boldsymbol{\theta}^*\|^2}$ for small $c > 0$, $T = \Omega(\log d)$

Output: $\tilde{\boldsymbol{\theta}}$

1: **Initialization:**
2: $\kappa_{\mathrm{sq}} = \frac{1}{3}\left(\sqrt{2}\sqrt{\frac{1}{m}\sum_{i=1}^m y_i^2 - \left(\frac{1}{m}\sum_{i=1}^m y_i\right)^2} + \frac{1}{m}\sum_{i=1}^m y_i\right)$
3: **if** $\kappa_{\mathrm{sq}} \leq 0$ **then**
4:    **return** $\tilde{\boldsymbol{\theta}} = 0$
5: **else**
6:    $\tilde{\boldsymbol{\theta}}^0 = \sqrt{\kappa_{\mathrm{sq}}}\boldsymbol{u}$ (where $\boldsymbol{u}$ is uniformly distributed over the unit sphere).
7:    **for** $t = 1, \ldots, T$ **do**
8:        $\tilde{\boldsymbol{\theta}}^{t+1} = \tilde{\boldsymbol{\theta}}^t - \mu\nabla_{\boldsymbol{\theta}}f_U(\tilde{\boldsymbol{\theta}}^t)$.
9:    **end for**
10:    **return** $\tilde{\boldsymbol{\theta}} = \tilde{\boldsymbol{\theta}}^{T+1}$.
11: **end if**

Theorem 2. *Under Assumption 1, if $n = \Omega\big(d\operatorname{polylog}(d)\big)$ and $\bar{\eta} > -3\|\boldsymbol{\theta}^*\|^2$, then there exists $\tilde{T} = \mathcal{O}(\log d)$ such that with probability at least $1 - \mathcal{O}\big(n^2 \exp(-1.5d)\big) - \mathcal{O}\big(n^{-9}\big)$, the iterates $\tilde{\boldsymbol{\theta}}^t$ of Algorithm 3 satisfy*

- *$\tilde{\boldsymbol{\theta}}^t$ converges linearly to $\kappa\boldsymbol{\theta}^*$ for all $t \geq \tilde{T}$, i.e.,*

$$d(\tilde{\boldsymbol{\theta}}^t, \kappa\boldsymbol{\theta}^*) \leq \left(1 - \frac{\mu}{2}\|\boldsymbol{\theta}^*\|^2\right)^{t-\tilde{T}}\|\boldsymbol{\theta}^*\|, \quad \forall t \geq \tilde{T} .$$

- *The ratio of the signal component $a_t := |\langle \boldsymbol{\theta}^t, \kappa\boldsymbol{\theta}^*\rangle|$ to the orthogonal component $b_t := \|\boldsymbol{\theta}^t - \frac{\langle \boldsymbol{\theta}^t, \kappa\boldsymbol{\theta}^*\rangle}{\|\boldsymbol{\theta}^*\|}\boldsymbol{\theta}^*\|$ obeys*

$$\frac{a_t}{b_t} \geq \frac{c_2}{\sqrt{d\log d}}(1 + c_1\mu^2)^t, \quad t = 0, 1, \ldots$$

for some universal constants $c_1, c_2 > 0$.

The second point of Theorem 2 implies that the ratio of the signal strength to the strength of its orthogonal component grows as the iteration count increases. This ensures that the signal can be identified eventually as $t \to \infty$. The proof of Theorem 2 builds on Chen et al. (2019) but some changes are needed to handle the corruptions.

8 Conclusion

In this paper, we derived convergence rate guarantees for ALT-MIN-PHASE, which is specifically designed for the phase retrieval problem under a strong corruption model. Our methodology facilitates signal recovery when $k = \mathcal{O}(n^{1-p})$ for any $p \in (0, 1]$, with only $\Omega(d\operatorname{polylog}(d))$ measurements. Moreover, we provide an efficient construction of LSQ-PHASE-ORACLE under a slightly less stringent corruption model. Future research could explore extending our analysis to regimes with constant corruption proportions under Assumption 1. It would also be interesting to investigate oracles that do not require Assumption 1.

References

Adler, R. J. (1990). An introduction to continuity, extrema, and related topics for general gaussian processes. *IMS*.

Bahmani, S. and Romberg, J. (2017). Phase retrieval meets statistical learning theory: A flexible convex relaxation. In *Artificial Intelligence and Statistics*, pages 252–260. PMLR.

Bakshi, A. and Prasad, A. (2021). Robust linear regression: Optimal rates in polynomial time. In *Proceedings of the 53rd Annual ACM SIGACT Symposium on Theory of Computing*, pages 102–115.

Candès, E. J. and Li, X. (2014). Solving quadratic equations via phaselift when there are about as many equations as unknowns. *Foundations of Computational Mathematics*, 14:1017–1026.

Candes, E. J., Li, X., and Soltanolkotabi, M. (2015). Phase retrieval via wirtinger flow: Theory and algorithms. *IEEE Transactions on Information Theory*, 61(4):1985–2007.

Candes, E. J., Strohmer, T., and Voroninski, V. (2013). Phaselift: Exact and stable signal recovery from magnitude measurements via convex programming. *Communications on Pure and Applied Mathematics*, 66(8):1241–1274.

Chen, S., Koehler, F., Moitra, A., and Yau, M. (2022). Online and distribution-free robustness: Regression and contextual bandits with huber contamination. In *2021 IEEE 62nd Annual Symposium on Foundations of Computer Science (FOCS)*, pages 684–695. IEEE.

Chen, Y. and Candes, E. (2015). Solving random quadratic systems of equations is nearly as easy as solving linear systems. *Advances in Neural Information Processing Systems*, 28.

Chen, Y., Chi, Y., Fan, J., and Ma, C. (2019). Gradient descent with random initialization: Fast global convergence for nonconvex phase retrieval. *Mathematical Programming*, 176:5–37.

Chen, Y., Chi, Y., and Goldsmith, A. J. (2015). Exact and stable covariance estimation from quadratic sampling via convex programming. *IEEE Transactions on Information Theory*, 61(7):4034–4059.

Demanet, L. and Hand, P. (2014). Stable optimizationless recovery from phaseless linear measurements. *Journal of Fourier Analysis and Applications*, 20:199–221.

Diakonikolas, I., Kong, W., and Stewart, A. (2019). Efficient algorithms and lower bounds for robust linear regression. In *Proceedings of the Thirtieth Annual ACM-SIAM Symposium on Discrete Algorithms*, pages 2745–2754. SIAM.

Dong, J., Valzania, L., Maillard, A., Pham, T.-a., Gigan, S., and Unser, M. (2023). Phase retrieval: From computational imaging to machine learning: A tutorial. *IEEE Signal Processing Magazine*, 40(1):45–57.

Fienup, J. R. (1982). Phase retrieval algorithms: a comparison. *Applied optics*, 21(15):2758–2769.

Gao, C. (2020). Robust regression via mutivariate regression depth. *Bernoulli*.

Ge, R., Huang, F., Jin, C., and Yuan, Y. (2015). Escaping from saddle points—online stochastic gradient for tensor decomposition. In *Conference on learning theory*, pages 797–842. PMLR.

Goldstein, T. and Studer, C. (2018). Phasemax: Convex phase retrieval via basis pursuit. *IEEE Transactions on Information Theory*, 64(4):2675–2689.

Hand, P. (2017). Phaselift is robust to a constant fraction of arbitrary errors. *Applied and Computational Harmonic Analysis*, 42(3):550–562.

Hoeffding, W. (1994). Probability inequalities for sums of bounded random variables. *The collected works of Wassily Hoeffding*, pages 409–426.

Huang, G., Li, S., and Xu, H. (2023). Robust outlier bound condition to phase retrieval with adversarial sparse outliers. *arXiv preprint arXiv:2311.13219*.

Jambulapati, A., Li, J., and Tian, K. (2020). Robust sub-gaussian principal component analysis and width-independent schatten packing. *Advances in Neural Information Processing Systems*, 33:15689–15701.

Jin, C., Ge, R., Netrapalli, P., Kakade, S. M., and Jordan, M. I. (2017). How to escape saddle points efficiently. In *International conference on machine learning*, pages 1724–1732. PMLR.

Kamath, G. (2015). Bounds on the expectation of the maximum of samples from a gaussian. *URL http://www. gautamkamath. com/writings/gaussian max. pdf*, 10(20-30):31.

Millane, R. P. (1990). Phase retrieval in crystallography and optics. *JOSA A*, 7(3):394–411.

Murray, R., Swenson, B., and Kar, S. (2017). Revisiting normalized gradient descent: Evasion of saddle points. *arXiv preprint arXiv:1711.05224*.

Nesterov, Y. and Polyak, B. T. (2006). Cubic regularization of newton method and its global performance. *Mathematical programming*, 108(1):177–205.

Netrapalli, P., Jain, P., and Sanghavi, S. (2013). Phase retrieval using alternating minimization. *Advances in Neural Information Processing Systems*, 26.

Stefik, M. (1978). Inferring dna structures from segmentation data. *Artificial Intelligence*, 11(1-2):85–114.

Sun, J., Qu, Q., and Wright, J. (2018). A geometric analysis of phase retrieval. *Foundations of Computational Mathematics*, 18:1131–1198.

Tan, Y. S. and Vershynin, R. (2023). Online stochastic gradient descent with arbitrary initialization solves non-smooth, non-convex phase retrieval. *Journal of Machine Learning Research*, 24(58):1–47.

Vershynin, R. (2010). Introduction to the non-asymptotic analysis of random matrices. *arXiv preprint arXiv:1011.3027*.

Waldspurger, I., d'Aspremont, A., and Mallat, S. (2015). Phase recovery, maxcut and complex semidefinite programming. *Mathematical Programming*, 149:47–81.

Walther, A. (1963). The question of phase retrieval in optics. *Optica Acta: International Journal of Optics*, 10(1):41–49.

Wang, G., Giannakis, G. B., and Eldar, Y. C. (2017). Solving systems of random quadratic equations via truncated amplitude flow. *IEEE Transactions on Information Theory*, 64(2):773–794.

Weller, D. S., Pnueli, A., Divon, G., Radzyner, O., Eldar, Y. C., and Fessler, J. A. (2015). Undersampled phase retrieval with outliers. *IEEE transactions on computational imaging*, 1(4):247–258.

Zhang, H., Chi, Y., and Liang, Y. (2016a). Provable non-convex phase retrieval with outliers: Median truncated-wirtinger flow. In *International conference on machine learning*, pages 1022–1031. PMLR.

Zhang, H., Zhou, Y., Liang, Y., and Chi, Y. (2016b). Reshaped wirtinger flow and incremental algorithm for solving quadratic system of equations. *arXiv preprint arXiv:1605.07719*.

A   Proof of Theorem 1

Theorem 1. *Let $S = \{(\boldsymbol{x}_i, y_i)\}_{i=1}^n$ be a set of measurements generated by the strong corruption model with corruption proportion $\epsilon = \frac{k}{n}$. We further assume that $k \in \mathcal{K}$. Let $n = \Omega\big(\frac{d\,\mathrm{polylog}(d) + \log(\frac{1}{\delta})}{\epsilon^2 \log(\frac{1}{\epsilon})}\big)$ for some $\delta \in (0, 1]$. With probability at least $1 - \delta - \mathcal{O}(\frac{1}{n})$, Algorithm 2 with parameters k and $\beta = \epsilon^2$ terminates within $\mathcal{O}(\frac{\sum_{i=1}^n y_i^2}{4(n-k)\epsilon^2})$ iterations, and outputs an estimate $\hat{\boldsymbol{\theta}}$ such that for some absolute constants $C_1, C_2, C_3 > 0$*

$$d(\hat{\boldsymbol{\theta}}, \boldsymbol{\theta}^*) \le 1.2 \max \left\{ \big(\psi(k, n, \boldsymbol{\eta})\big)^{\frac{1}{2}}, \psi(k, n, \boldsymbol{\eta}) \right\} \sqrt{\epsilon} \,,$$

where $\psi(k, n, \boldsymbol{\eta}) = \frac{\sqrt{(C_1 + \max_i |\eta_i|)(1 + \Delta)}}{(1 - 3\epsilon)(C_2 - \Delta) - C_3\Delta}$.

In this section, we provide the detailed proofs for the lemmas discussed in Section 6. Due to the rotational invariance of the Gaussian distribution, it is sufficient to demonstrate the results for $\boldsymbol{\theta}^* = [1, 0, \ldots, 0]^\top$. This is similar to the approaches employed by Chen et al. (2019) and Sun et al. (2018).

For a fixed $U \subset [n]$ with $|U| = (1 - 2\epsilon)n$, we restate the following definitions (along with the Hessian) from Section 6:

$$f_U(\boldsymbol{\theta}) = \frac{1}{4|U|} \sum_{i \in U} \left(\langle \boldsymbol{x}_i, \boldsymbol{\theta} \rangle^2 - y_i\right)^2 \tag{6}$$

$$\nabla f_U(\boldsymbol{\theta}) = \frac{1}{|U|} \sum_{i \in U} \left(\langle \boldsymbol{x}_i, \boldsymbol{\theta} \rangle^2 - y_i\right) \boldsymbol{x}_i \boldsymbol{x}_i^\top \boldsymbol{\theta}$$

$$\nabla^2 f_U(\boldsymbol{\theta}) = \frac{1}{|U|} \sum_{i \in U} \left(3\langle \boldsymbol{x}_i, \boldsymbol{\theta} \rangle^2 - y_i\right) \boldsymbol{x}_i \boldsymbol{x}_i^\top \,.$$

For ease of notation, when it does not introduce ambiguity, we reindex the elements in U to $\{1, \ldots, m\}$, where $m = (1 - 2\epsilon)n$.

A.1   Preprocessing Step

Initially, observe that, by Corollary 1, at most k of the y_i's can attain values of $\omega(\log n)$ with probability at least $1 - \mathcal{O}\left(\frac{1}{n}\right)$. Consequently, the preprocessing step not only removes any y_i's with negative values but also eliminates y_i's that are of the order $\omega(\log n)$. This ensures that the remaining η_i's are constrained to be of the order $\mathcal{O}(\log n)$. Next, we prove Lemma 2.

A.2 Proof of Lemma 2

Lemma 2. *If $\boldsymbol{\theta}$ lies on the line segment connecting $\hat{\boldsymbol{\theta}}$ and $\boldsymbol{\theta}^*$ and $n = \Omega\big(\frac{d\operatorname{polylog}(d)+\log(\frac{1}{\delta})}{\epsilon^2 \log(\frac{1}{\epsilon})}\big)$ for some $\delta \in (0,1]$, then with probability at least $1 - \delta - \mathcal{O}(\frac{1}{n})$,*

$$(\hat{\boldsymbol{\theta}} - \boldsymbol{\theta}^*)^\top \nabla^2 f_{\hat{U}}(\boldsymbol{\theta})(\hat{\boldsymbol{\theta}} - \boldsymbol{\theta}^*) \le 2L(\hat{\boldsymbol{\theta}}, \boldsymbol{\theta}^*, \Delta, \boldsymbol{\eta})\|\hat{\boldsymbol{\theta}} - \boldsymbol{\theta}^*\|^2.$$

Proof. We define $\boldsymbol{z} = \frac{\hat{\boldsymbol{\theta}} - \boldsymbol{\theta}^*}{\|\hat{\boldsymbol{\theta}} - \boldsymbol{\theta}^*\|}$. Let $\bar{\boldsymbol{\theta}}$ be a point in the line-segment connecting $\hat{\boldsymbol{\theta}}$ and $\boldsymbol{\theta}^*$. This implies that there exists a $\bar{\lambda} \in [0,1]$ such that

$$\bar{\boldsymbol{\theta}} = (1 - \bar{\lambda})\hat{\boldsymbol{\theta}} + \bar{\lambda}\boldsymbol{\theta}^* .$$

Therefore,

$$\bar{\boldsymbol{\theta}} - \boldsymbol{\theta}^* = (1 - \bar{\lambda})(\hat{\boldsymbol{\theta}} - \boldsymbol{\theta}^*) . \tag{7}$$

Using the expression from (6) and substituting y_i from data generation model 1, we can write:

$$\boldsymbol{z}^\top \nabla^2 f_{\hat{U}}(\bar{\boldsymbol{\theta}})\boldsymbol{z} = \frac{1}{m}\sum_{i=1}^m \big(3\langle \boldsymbol{x}_i, \bar{\boldsymbol{\theta}}\rangle^2 - \langle \boldsymbol{x}_i, \boldsymbol{\theta}^*\rangle^2 - \eta_i\big)\boldsymbol{z}^\top \boldsymbol{x}_i \boldsymbol{x}_i^\top \boldsymbol{z}$$

After some algebraic manipulation, this can be rewritten as:

$$\boldsymbol{z}^\top \nabla^2 f_{\hat{U}}(\bar{\boldsymbol{\theta}})\boldsymbol{z} = \frac{1}{m}\sum_{i=1}^m \big(3(\langle \boldsymbol{x}_i, \bar{\boldsymbol{\theta}}\rangle - \langle \boldsymbol{x}_i, \boldsymbol{\theta}^*\rangle)^2 + 6(\langle \boldsymbol{x}_i, \bar{\boldsymbol{\theta}}\rangle - \langle \boldsymbol{x}_i, \boldsymbol{\theta}^*\rangle)\langle \boldsymbol{x}_i, \boldsymbol{\theta}^*\rangle) + 2\langle \boldsymbol{x}_i, \boldsymbol{\theta}^*\rangle^2 - \eta_i\big)\boldsymbol{z}^\top \boldsymbol{x}_i \boldsymbol{x}_i^\top \boldsymbol{z}$$

Substituting the definition of $\boldsymbol{z}$ and the result from (7), we get:

$$\boldsymbol{z}^\top \nabla^2 f_{\hat{U}}(\bar{\boldsymbol{\theta}})\boldsymbol{z} = \frac{1}{m}\sum_{i=1}^m \big(3(1-\bar{\lambda})^2\langle \boldsymbol{x}_i, \boldsymbol{z}\rangle^2\|\hat{\boldsymbol{\theta}} - \boldsymbol{\theta}^*\|^2 + 6(1-\bar{\lambda})\langle \boldsymbol{x}_i, \boldsymbol{z}\rangle x_{i1}\|\hat{\boldsymbol{\theta}} - \boldsymbol{\theta}^*\| + 2x_{i1}^2 - \eta_i\big)\boldsymbol{z}^\top \boldsymbol{x}_i \boldsymbol{x}_i^\top \boldsymbol{z}$$

$$= \frac{1}{m}\sum_{i=1}^m \big(3(1-\bar{\lambda})^2\langle \boldsymbol{x}_i, \boldsymbol{z}\rangle^4\|\hat{\boldsymbol{\theta}} - \boldsymbol{\theta}^*\|^2 + 6(1-\bar{\lambda})\langle \boldsymbol{x}_i, \boldsymbol{z}\rangle^3 x_{i1}\|\hat{\boldsymbol{\theta}} - \boldsymbol{\theta}^*\| + 2\langle \boldsymbol{x}_i, \boldsymbol{z}\rangle^2 x_{i1}^2 - \eta_i\langle \boldsymbol{x}_i, \boldsymbol{z}\rangle^2\big)$$

Recall that $\Delta = \epsilon\sqrt{\log \epsilon^{-1}}\log^2(\epsilon n)$. Utilizing the results from Lemma 9 and Cauchy-Schwartz inequality, with probability at least $1 - \delta - \mathcal{O}(\frac{1}{n})$:

$$\boldsymbol{z}^\top \nabla^2 f_{\hat{U}}(\bar{\boldsymbol{\theta}})\boldsymbol{z} \le (1-\bar{\lambda})^2(C_{40} + \Delta)\|\hat{\boldsymbol{\theta}} - \boldsymbol{\theta}^*\|^2 + (1-\bar{\lambda})(C_{31} + \Delta)\|\hat{\boldsymbol{\theta}} - \boldsymbol{\theta}^*\| + (C_{22} + \Delta) + \max_i |\eta_i|(1+\Delta)$$

$$\le (C_{40} + \Delta)\|\hat{\boldsymbol{\theta}} - \boldsymbol{\theta}^*\|^2 + (C_{31} + \Delta)\|\hat{\boldsymbol{\theta}} - \boldsymbol{\theta}^*\| + (C_{22} + \Delta) + \max_i |\eta_i|(1+\Delta)$$

$$= 2L(\hat{\boldsymbol{\theta}}, \boldsymbol{\theta}^*, \Delta, \boldsymbol{\eta}) .$$

$\square$

A.3 Proof of Lemma 3

Lemma 3. *Let $\bar{\boldsymbol{\theta}}$ be any point on the line segment connecting $\hat{\boldsymbol{\theta}}$ and $\boldsymbol{\theta}^*$. Assume that the following properties hold:*

1. *$\langle \nabla f_{\hat{U}}(\hat{\boldsymbol{\theta}}), \hat{\boldsymbol{\theta}} - \boldsymbol{\theta}^*\rangle \ge \gamma\|\hat{\boldsymbol{\theta}} - \boldsymbol{\theta}^*\| > 0$ and*

2. *$\frac{\hat{\boldsymbol{\theta}} - \boldsymbol{\theta}^*}{\|\hat{\boldsymbol{\theta}} - \boldsymbol{\theta}^*\|}\nabla^2 f_{\hat{U}}(\bar{\boldsymbol{\theta}})\frac{\hat{\boldsymbol{\theta}} - \boldsymbol{\theta}^*}{\|\hat{\boldsymbol{\theta}} - \boldsymbol{\theta}^*\|} \le 2L(\hat{\boldsymbol{\theta}}, \boldsymbol{\theta}^*, \Delta, \boldsymbol{\eta}).$*

Then, there exists $\boldsymbol{\theta} \in \mathbb{R}^d$ such that

$$f_{\hat{U}}(\boldsymbol{\theta}) \le f_{\hat{U}}(\hat{\boldsymbol{\theta}}) - \frac{\gamma^2}{4L(\hat{\boldsymbol{\theta}}, \boldsymbol{\theta}^*, \Delta, \boldsymbol{\eta})} .$$

Proof. Consider a $\boldsymbol{\theta} = (1 - \lambda)\hat{\boldsymbol{\theta}} + \lambda\boldsymbol{\theta}^*$, where $\lambda \in [0, 1]$. Note that $\boldsymbol{\theta} - \hat{\boldsymbol{\theta}} = \lambda(\boldsymbol{\theta}^* - \hat{\boldsymbol{\theta}})$. Using Taylor's theorem, we can write

$$f_{\hat{U}}(\boldsymbol{\theta}) = f_{\hat{U}}(\hat{\boldsymbol{\theta}}) + \langle \nabla f_{\hat{U}}(\hat{\boldsymbol{\theta}}), \boldsymbol{\theta} - \hat{\boldsymbol{\theta}} \rangle + \frac{1}{2}(\boldsymbol{\theta} - \hat{\boldsymbol{\theta}})^\top \nabla^2 f_{\hat{U}}(\bar{\boldsymbol{\theta}})(\boldsymbol{\theta} - \hat{\boldsymbol{\theta}}),$$

for some $\bar{\boldsymbol{\theta}}$ in the line-segment joining $\boldsymbol{\theta}$ and $\hat{\boldsymbol{\theta}}$. It follows that $\bar{\boldsymbol{\theta}}$ also lies in the line-segment joining $\hat{\boldsymbol{\theta}}$ and θ^*. Thus,

$$f_{\hat{U}}(\boldsymbol{\theta}) \leq f_{\hat{U}}(\hat{\boldsymbol{\theta}}) - \lambda\gamma\|\hat{\boldsymbol{\theta}} - \boldsymbol{\theta}^*\| + L(\hat{\boldsymbol{\theta}}, \boldsymbol{\theta}^*, \Delta, \boldsymbol{\eta})\lambda^2\|\hat{\boldsymbol{\theta}} - \boldsymbol{\theta}^*\|^2$$
$$\leq f_{\hat{U}}(\hat{\boldsymbol{\theta}}) - \frac{\gamma^2}{4L(\hat{\boldsymbol{\theta}}, \boldsymbol{\theta}^*, \Delta, \boldsymbol{\eta})}.$$

The final step follows by picking $\lambda = \frac{\gamma}{2L(\hat{\boldsymbol{\theta}}, \boldsymbol{\theta}^*, \Delta, \boldsymbol{\eta})\|\hat{\boldsymbol{\theta}} - \boldsymbol{\theta}^*\|}$. $\qquad\square$

As outlined in Section 6, Lemma 1 follows from combining the results of Lemma 2 and Lemma 3. This establishes that $\hat{\boldsymbol{\theta}}$ is an $2\sqrt{L(\hat{\boldsymbol{\theta}}, \boldsymbol{\theta}^*, \Delta, \boldsymbol{\eta})}\epsilon$-stationary point of $f_{\hat{U}}(\boldsymbol{\theta})$ with probability at least $1 - \delta - \mathcal{O}(\frac{1}{n})$. We now proceed to analyze the proximity of $\hat{\boldsymbol{\theta}}$ to $\boldsymbol{\theta}^*$. For simplicity, we consider $d(\boldsymbol{\theta}, \boldsymbol{\theta}^*)$ as $\|\boldsymbol{\theta} - \boldsymbol{\theta}^*\|$, without loss of generality, by potentially flipping the sign of $\boldsymbol{\theta}^*$. Following the arguments from Section 6, our first task is to prove Lemma 4.

A.4 Proof of Lemma 4

Lemma 4. *If* $n = \Omega\big(\frac{d\,\mathrm{polylog}(d) + \log(\frac{1}{\delta})}{\epsilon^2 \log(\frac{1}{\epsilon})}\big)$ *for some* $\delta \in (0, 1]$, *then for some absolute constants* C_1, C_2 *and* $C_3 > 0$, *the following holds with probability at least* $1 - \delta - \mathcal{O}(\frac{1}{n})$:

$$\zeta(\hat{\boldsymbol{\theta}}, \boldsymbol{\theta}^*, n, k) \geq (1 - 3\epsilon)\Big((C_1 - \Delta)\|\hat{\boldsymbol{\theta}} - \boldsymbol{\theta}^*\|^4 + (C_2 - \Delta)\|\hat{\boldsymbol{\theta}} - \boldsymbol{\theta}^*\|^3 + (C_3 - \Delta)\|\hat{\boldsymbol{\theta}} - \boldsymbol{\theta}^*\|^2\Big).$$

Proof. Recall that

$$\zeta(\hat{\boldsymbol{\theta}}, \boldsymbol{\theta}^*, n, k) = \frac{1}{n}\sum_{i \in U^* \cap \hat{U}} \big(\langle \boldsymbol{x}_i, \hat{\boldsymbol{\theta}} \rangle^2 - \langle \boldsymbol{x}_i, \boldsymbol{\theta}^* \rangle^2\big)\boldsymbol{x}_i^\top\hat{\boldsymbol{\theta}}(\hat{\boldsymbol{\theta}} - \boldsymbol{\theta}^*)^\top\boldsymbol{x}_i$$

We rewrite it in the following way.

$$\frac{1}{n}\sum_{i \in U^* \cap \hat{U}} \big(\langle \boldsymbol{x}_i, \hat{\boldsymbol{\theta}} \rangle^2 - \langle \boldsymbol{x}_i, \boldsymbol{\theta}^* \rangle^2\big)\boldsymbol{x}_i^\top\hat{\boldsymbol{\theta}}(\hat{\boldsymbol{\theta}} - \boldsymbol{\theta}^*)^\top\boldsymbol{x}_i$$
$$= \frac{1}{n}\sum_{i \in U^* \cap \hat{U}} \left(\langle \boldsymbol{x}_i, \hat{\boldsymbol{\theta}} - \boldsymbol{\theta}^* \rangle^4 + 4\langle \boldsymbol{x}_i, \hat{\boldsymbol{\theta}} - \boldsymbol{\theta}^* \rangle^2\langle \boldsymbol{x}_i, \boldsymbol{\theta}^* \rangle^2 + 4\langle \boldsymbol{x}_i, \hat{\boldsymbol{\theta}} - \boldsymbol{\theta}^* \rangle^3\langle \boldsymbol{x}_i, \boldsymbol{\theta}^* \rangle\right)$$
$$= \frac{1}{n}\sum_{i \in U^* \cap \hat{U}} \left(\langle \boldsymbol{x}_i, \boldsymbol{z} \rangle^4\|\boldsymbol{\theta}^* - \hat{\boldsymbol{\theta}}\|^4 + 4\langle \boldsymbol{x}_i, \boldsymbol{z} \rangle^2 x_{i1}^2\|\boldsymbol{\theta}^* - \hat{\boldsymbol{\theta}}\|^2 + 4\langle \boldsymbol{x}_i, \boldsymbol{z} \rangle^3 x_{i1}\|\boldsymbol{\theta}^* - \hat{\boldsymbol{\theta}}\|^3\right),$$

where the last equality is by defining $\boldsymbol{z} = \frac{\hat{\boldsymbol{\theta}} - \boldsymbol{\theta}^*}{\|\hat{\boldsymbol{\theta}} - \boldsymbol{\theta}^*\|}$. Note that $|U^* \cap \hat{U}| \geq (1 - 3\epsilon)n$ and using the result from Lemma 9, we can write that with probability at least $1 - \delta - \mathcal{O}\big(\frac{1}{n}\big)$,

$$\zeta(\hat{\boldsymbol{\theta}}, \boldsymbol{\theta}^*, n, k) \geq (1 - 3\epsilon)\Big((C_{40} - \Delta)\|\boldsymbol{\theta}^* - \hat{\boldsymbol{\theta}}\|^4 + (C_{22} - \Delta)\|\boldsymbol{\theta}^* - \hat{\boldsymbol{\theta}}\|^2 + (C_{31} - \Delta)\|\boldsymbol{\theta}^* - \hat{\boldsymbol{\theta}}\|^3\Big)$$

$\qquad\square$

A.5 Proof of Lemma 5

Recall that

$$\xi(\hat{\boldsymbol{\theta}}, \boldsymbol{\theta}^*, n, k, \boldsymbol{\eta}) = -\frac{1}{n}\sum_{i \in \hat{U} \cap C^*} \left(\langle \boldsymbol{x}_i, \hat{\boldsymbol{\theta}} \rangle^2 - y_i\right)\boldsymbol{x}_i^\top\hat{\boldsymbol{\theta}}(\hat{\boldsymbol{\theta}} - \boldsymbol{\theta}^*)^\top\boldsymbol{x}_i$$

14

Using the Cauchy-Schwartz inequality,

$$\xi(\hat{\boldsymbol{\theta}}, \boldsymbol{\theta}^*, n, k, \boldsymbol{\eta}) \leq \underbrace{\left(\frac{1}{n} \sum_{i \in \hat{U} \cap C^*} \left(\langle \boldsymbol{x}_i, \hat{\boldsymbol{\theta}} \rangle^2 - y_i \right)^2 \right)^{\frac{1}{2}}}_{\xi_1(\hat{\boldsymbol{\theta}}, \boldsymbol{\theta}^*, n, k, \boldsymbol{\eta})} \times \underbrace{\left(\frac{1}{n} \sum_{i \in \hat{U} \cap C^*} \left(\boldsymbol{x}_i^\top \hat{\boldsymbol{\theta}} (\hat{\boldsymbol{\theta}} - \boldsymbol{\theta}^*)^\top \boldsymbol{x}_i \right)^2 \right)^{\frac{1}{2}}}_{\xi_2(\hat{\boldsymbol{\theta}}, \boldsymbol{\theta}^*, n, k)}.$$

For a fixed $\hat{\boldsymbol{\theta}}$, Algorithm 2 outputs $\hat{U}$ that yields the smallest loss. This implies that

$$\frac{1}{n} \sum_{i \in \hat{U}} \left(\langle \boldsymbol{x}_i, \hat{\boldsymbol{\theta}} \rangle^2 - y_i \right)^2 \leq \frac{1}{n} \sum_{i \in U^*} \left(\langle \boldsymbol{x}_i, \hat{\boldsymbol{\theta}} \rangle^2 - y_i \right)^2.$$

By removing the measurements belonging to $\hat{U} \cap U^*$ from both $\hat{U}$ and U^*, we obtain

$$\xi_1(\hat{\boldsymbol{\theta}}, \boldsymbol{\theta}^*, n, k, \boldsymbol{\eta}) = \frac{1}{n} \sum_{i \in \hat{U} \cap C^*} \left(\langle \boldsymbol{x}_i, \hat{\boldsymbol{\theta}} \rangle^2 - y_i \right)^2 \leq \frac{1}{n} \sum_{i \in U^* \setminus \hat{U}} \left(\langle \boldsymbol{x}_i, \hat{\boldsymbol{\theta}} \rangle^2 - y_i \right)^2. \tag{8}$$

Note that the right-hand side of (8) contains terms that represent uncorrupted measurements. This allows us to provide an upper bound on $\xi_1(\hat{\boldsymbol{\theta}}, \boldsymbol{\theta}^*, n, k, \boldsymbol{\eta})$ that is independent of $\boldsymbol{\eta}$. Similarly, $\xi_2(\hat{\boldsymbol{\theta}}, \boldsymbol{\theta}^*, n, k)$ does not involve any y_i and thus remains unaffected by the corrupted measurements. Now we are ready to prove Lemma 5.

Lemma 5. *Let $n = \Omega\left(\frac{d \operatorname{polylog}(d) + \log(\frac{1}{\delta})}{\epsilon^2 \log(\frac{1}{\epsilon})} \right)$ for some $\delta \in (0, 1]$ and for some absolute constants C_1, C_2 and $C_3 > 0$, define*

$$\upsilon(\hat{\boldsymbol{\theta}}, \boldsymbol{\theta}^*, n, k) := C_1 \Delta \| \hat{\boldsymbol{\theta}} - \boldsymbol{\theta}^* \|^4 + C_2 \Delta \| \hat{\boldsymbol{\theta}} - \boldsymbol{\theta}^* \|^3 + C_3 \Delta \| \hat{\boldsymbol{\theta}} - \boldsymbol{\theta}^* \|^2.$$

Then, with probability at least $1 - \delta - \mathcal{O}(\frac{1}{n})$:

1. *$\xi_1(\hat{\boldsymbol{\theta}}, \boldsymbol{\theta}^*, n, k, \boldsymbol{\eta}) \leq \upsilon(\hat{\boldsymbol{\theta}}, \boldsymbol{\theta}^*, n, k)$*

2. *$\xi_2(\hat{\boldsymbol{\theta}}, \boldsymbol{\theta}^*, n, k) \leq \upsilon(\hat{\boldsymbol{\theta}}, \boldsymbol{\theta}^*, n, k)$*

3. *Consequently, $\xi(\hat{\boldsymbol{\theta}}, \boldsymbol{\theta}^*, n, k, \boldsymbol{\eta}) \leq \upsilon(\hat{\boldsymbol{\theta}}, \boldsymbol{\theta}^*, n, k)$.*

Proof. We start by bounding $\xi_1(\hat{\boldsymbol{\theta}}, \boldsymbol{\theta}^*, n, k, \boldsymbol{\eta})$.

A.5.1   Upper bound ξ_1.

We showed in (8) that,

$$\frac{1}{n} \sum_{i \in \hat{U} \cap C^*} \left(\langle \boldsymbol{x}_i, \hat{\boldsymbol{\theta}} \rangle^2 - y_i \right)^2 \leq \frac{1}{n} \sum_{i \in U^* \setminus \hat{U}} \left(\langle \boldsymbol{x}_i, \hat{\boldsymbol{\theta}} \rangle^2 - \langle \boldsymbol{x}_i, \boldsymbol{\theta}^* \rangle^2 \right)^2$$

$$= \frac{1}{n} \sum_{i \in U^* \setminus \hat{U}} \left(\langle \boldsymbol{x}_i, \hat{\boldsymbol{\theta}} - \boldsymbol{\theta}^* \rangle^4 + 4 \langle \boldsymbol{x}_i, \hat{\boldsymbol{\theta}} - \boldsymbol{\theta}^* \rangle^2 \langle \boldsymbol{x}_i, \boldsymbol{\theta}^* \rangle^2 + 4 \langle \boldsymbol{x}_i, \hat{\boldsymbol{\theta}} - \boldsymbol{\theta}^* \rangle^3 \langle \boldsymbol{x}_i, \boldsymbol{\theta}^* \rangle \right)$$

$$= \frac{1}{n} \sum_{i \in U^* \setminus \hat{U}} \left(\langle \boldsymbol{x}_i, \boldsymbol{z} \rangle^4 \| \boldsymbol{\theta}^* - \hat{\boldsymbol{\theta}} \|^4 + 4 \langle \boldsymbol{x}_i, \boldsymbol{z} \rangle^2 x_{i1}^2 \| \boldsymbol{\theta}^* - \hat{\boldsymbol{\theta}} \|^2 + 4 \langle \boldsymbol{x}_i, \boldsymbol{z} \rangle^3 x_{i1} \| \boldsymbol{\theta}^* - \hat{\boldsymbol{\theta}} \|^3 \right)$$

where we substitute $\boldsymbol{z} = \frac{\hat{\boldsymbol{\theta}} - \boldsymbol{\theta}^*}{\| \hat{\boldsymbol{\theta}} - \boldsymbol{\theta}^* \|}$ in the last equation. Note that $\left| U^* \setminus \hat{U} \right| \leq \epsilon n$. Using Lemma 10, we get

$$\xi_1(\hat{\boldsymbol{\theta}}, \boldsymbol{\theta}^*, n, k, \boldsymbol{\eta}) \leq D_{40} \Delta \| \boldsymbol{\theta}^* - \hat{\boldsymbol{\theta}} \|^4 + D_{22} \Delta \| \boldsymbol{\theta}^* - \hat{\boldsymbol{\theta}} \|^2 + D_{31} \Delta \| \boldsymbol{\theta}^* - \hat{\boldsymbol{\theta}} \|^3, \tag{9}$$

with probability at least $1 - \mathcal{O}(\delta) - \mathcal{O}\left(\frac{1}{n} \right)$ for some absolute constants $D_{40}, D_{22}, D_{31} > 0$. Next, we provide an upper bound on $\xi_2(\hat{\boldsymbol{\theta}}, \boldsymbol{\theta}^*, n, k)$.

Upper bound on $\xi_2(\hat{\boldsymbol{\theta}}, \boldsymbol{\theta}^*, n, k)$. By simple algebraic manipulation, we can write:

$$\xi_2(\hat{\boldsymbol{\theta}}, \boldsymbol{\theta}^*, n, k) = \frac{1}{n} \sum_{i \in C^* \cap \hat{U}} \left(\langle \boldsymbol{x}_i, \hat{\boldsymbol{\theta}} - \boldsymbol{\theta}^* \rangle^4 + \langle \boldsymbol{x}_i, \hat{\boldsymbol{\theta}} - \boldsymbol{\theta}^* \rangle^2 \langle \boldsymbol{x}_i, \boldsymbol{\theta}^* \rangle^2 + 2 \langle \boldsymbol{x}_i, \hat{\boldsymbol{\theta}} - \boldsymbol{\theta}^* \rangle^3 \langle \boldsymbol{x}_i, \boldsymbol{\theta}^* \rangle \right)$$

$$= \frac{1}{n} \sum_{i \in C^* \cap \hat{U}} \left(\langle \boldsymbol{x}_i, \boldsymbol{z} \rangle^4 \|\boldsymbol{\theta}^* - \hat{\boldsymbol{\theta}}\|^4 + \langle \boldsymbol{x}_i, \boldsymbol{z} \rangle^2 \boldsymbol{x}_{i1}^2 \|\boldsymbol{\theta}^* - \hat{\boldsymbol{\theta}}\|^2 + 2 \langle \boldsymbol{x}_i, \boldsymbol{z} \rangle^3 x_{i1} \|\boldsymbol{\theta}^* - \hat{\boldsymbol{\theta}}\|^3 \right),$$

where the last equation again uses $\boldsymbol{z} = \frac{\hat{\boldsymbol{\theta}} - \boldsymbol{\theta}^*}{\|\hat{\boldsymbol{\theta}} - \boldsymbol{\theta}^*\|}$. Observe that $|C^* \cap \hat{U}| \leq \epsilon n$. Using Lemma 10, we get

$$\xi_2(\hat{\boldsymbol{\theta}}, \boldsymbol{\theta}^*, n, k) \leq E_{40} \Delta \|\boldsymbol{\theta}^* - \hat{\boldsymbol{\theta}}\|^4 + E_{22} \Delta \|\boldsymbol{\theta}^* - \hat{\boldsymbol{\theta}}\|^2 + E_{31} \Delta \|\boldsymbol{\theta}^* - \hat{\boldsymbol{\theta}}\|^3, \tag{10}$$

with probability at least $1 - \mathcal{O}(\delta) - \mathcal{O}\left(\frac{1}{n}\right)$ for some absolute constants $E_{40}, E_{22}, E_{31} > 0$.

The final upper bound on $\xi(\hat{\boldsymbol{\theta}}, \boldsymbol{\theta}^*, n, k, \boldsymbol{\eta})$ simply combines (9) and (10). $\square$

We are now ready to put everything together. Recall that,

$$\zeta(\hat{\boldsymbol{\theta}}, \boldsymbol{\theta}^*, n, k) \leq \gamma \|\hat{\boldsymbol{\theta}} - \boldsymbol{\theta}^*\| + \xi(\hat{\boldsymbol{\theta}}, \boldsymbol{\theta}^*, n, k, \boldsymbol{\eta})$$

Recall from Lemma 1 that $\gamma = 2\sqrt{L(\hat{\boldsymbol{\theta}}, \boldsymbol{\theta}^*, \Delta, \boldsymbol{\eta})\epsilon}$ and

$$2L(\hat{\boldsymbol{\theta}}, \boldsymbol{\theta}^*, \Delta, \boldsymbol{\eta}) = (C_{40} + \Delta)\|\hat{\boldsymbol{\theta}} - \boldsymbol{\theta}^*\|^2 + (C_{31} + \Delta)\|\hat{\boldsymbol{\theta}} - \boldsymbol{\theta}^*\| + (C_{22} + \Delta) + \max_i |\eta_i|(1 + \Delta).$$

Substituting the lower bound on $\zeta(\hat{\boldsymbol{\theta}}, \boldsymbol{\theta}^*, n, k)$ and upper bound on $\xi(\hat{\boldsymbol{\theta}}, \boldsymbol{\theta}^*, n, k, \boldsymbol{\eta})$, we get:

$$(1 - 3\epsilon)\left((C_{40} - \Delta)\|\boldsymbol{\theta}^* - \hat{\boldsymbol{\theta}}\|^3 + (C_{22} - \Delta)\|\boldsymbol{\theta}^* - \hat{\boldsymbol{\theta}}\| + (C_{31} - \Delta)\|\boldsymbol{\theta}^* - \hat{\boldsymbol{\theta}}\|^2 \right)$$

$$\leq \sqrt{2\left((C_{40} + \Delta)\|\hat{\boldsymbol{\theta}} - \boldsymbol{\theta}^*\|^2 + (C_{31} + \Delta)\|\hat{\boldsymbol{\theta}} - \boldsymbol{\theta}^*\| + (C_{22} + \Delta) + \max_i |\eta_i|(1 + \Delta) \right)\epsilon}$$

$$+ F_{40} \Delta \|\boldsymbol{\theta}^* - \hat{\boldsymbol{\theta}}\|^3 + F_{22} \Delta \|\boldsymbol{\theta}^* - \hat{\boldsymbol{\theta}}\| + F_{31} \Delta \|\boldsymbol{\theta}^* - \hat{\boldsymbol{\theta}}\|^2,$$

where $F_{40}, F_{22}, F_{31} > 0$ are some appropriately chosen constants. To simplify this expression, we consider two regimes.

1. When $\|\boldsymbol{\theta}^* - \hat{\boldsymbol{\theta}}\| \leq 1$, for some absolute constants $H, G, I > 0$

$$(1 - 3\epsilon)(I - \Delta)\|\boldsymbol{\theta}^* - \hat{\boldsymbol{\theta}}\| \leq \sqrt{(H + \max_i |\eta_i|)(1 + \Delta)\epsilon} + G\Delta\|\boldsymbol{\theta}^* - \hat{\boldsymbol{\theta}}\|.$$

   We can further simplify this to

$$\|\boldsymbol{\theta}^* - \hat{\boldsymbol{\theta}}\| \leq \frac{\sqrt{(H + \max_i |\eta_i|)(1 + \Delta)}}{(1 - 3\epsilon)(I - \Delta) - G\Delta}\epsilon$$

2. Similarly, when $\|\boldsymbol{\theta}^* - \hat{\boldsymbol{\theta}}\| \geq 1$,

$$(1 - 3\epsilon)(C_{22} - \Delta)\|\boldsymbol{\theta}^* - \hat{\boldsymbol{\theta}}\|^3 \leq \sqrt{2\left((C_{40} + \Delta) + (C_{31} + \Delta) + (C_{22} + \Delta) + \max_i |\eta_i|(1 + \Delta) \right)\|\hat{\boldsymbol{\theta}} - \boldsymbol{\theta}^*\|\epsilon}$$

$$+ G\Delta\|\boldsymbol{\theta}^* - \hat{\boldsymbol{\theta}}\|^3$$

   Upon further simplification and for some absolute constant $H, G, I > 0$, we get:

$$(1 - 3\epsilon)(I - \Delta)\|\boldsymbol{\theta}^* - \hat{\boldsymbol{\theta}}\|^3 \leq \sqrt{2\left((H + \max_i |\eta_i|)(1 + \Delta) \right)\|\hat{\boldsymbol{\theta}} - \boldsymbol{\theta}^*\|\epsilon} + G\Delta\|\boldsymbol{\theta}^* - \hat{\boldsymbol{\theta}}\|^3$$

   This leads to:

$$\|\boldsymbol{\theta}^* - \hat{\boldsymbol{\theta}}\| \leq \sqrt{\frac{\sqrt{2\left((H + \max_i |\eta_i|)(1 + \Delta) \right)}}{(1 - 3\epsilon)(I - \Delta) - G\Delta}} \sqrt{\epsilon}.$$

Combining the results from both the regimes, we get

$$d(\hat{\boldsymbol{\theta}}, \boldsymbol{\theta}^*) \leq 1.2 \max\left\{ \left(\psi(k, n, \boldsymbol{\eta})\right)^{\frac{1}{2}}, \psi(k, n, \boldsymbol{\eta}) \right\} \sqrt{\epsilon},$$

where $\psi(k, n, \boldsymbol{\eta}) = \frac{\sqrt{(H + \max_i |\eta_i|)(1 + \Delta)}}{(1 - 3\epsilon)(I - \Delta) - G\Delta}$.

B Auxiliary Lemmas

In this section, we collect several auxiliary lemmas that are utilized throughout various parts of this paper.

Lemma 6 (Concentration of the max of Gaussian random variables)**.** *Let $a_i \sim \mathcal{N}(0, 1), i \in [n]$ be the n i.i.d. Gaussian random variables. Define $a := \max_{i \in [n]} a_i$. Then the following results hold:*

1. *The expected maximum of a, $\mathbb{E}[a]$ is $\Theta(\sqrt{\log n})$ (*Kamath, 2015*):*

$$\sqrt{\frac{\log n}{\pi \log 2}} \leq \mathbb{E}[a] \leq \sqrt{2 \log n}$$

2. *Borell-TIS inequality: the maximum of Gaussian is well-concentrated (*Adler, 1990*):*

$$\mathbb{P}\left[|a - \mathbb{E}[a]| \geq \sqrt{2 \log n}\right] \leq \frac{2}{n}$$

3. *Consequently, $|a| \leq \sqrt{8 \log n}$ with probability at least $1 - \frac{2}{n}$.*

The results of Lemma 6 naturally lead to several corollaries that will be utilized extensively throughout this work.

Corollary 1. *Let $a_i \sim \mathcal{N}(0, 1), i \in [n]$ be the n i.i.d. Gaussian random variables. Define $b_i := a_i^2$, and $b := \max_{i \in [n]} b_i$. Then,*

$$\mathbb{P}[b \geq 8 \log n] \leq \frac{2}{n}.$$

Proof. The result is a direct consequence of Lemma 6.

$$\mathbb{P}[b \geq 8 \log n] = \mathbb{P}\left[\max_{i \in [n]} a_i^2 \geq 8 \log n\right] = \mathbb{P}\left[\left(\max_{i \in [n]} |a_i|\right)^2 \geq 8 \log n\right]$$

$$= \mathbb{P}\left[\max_{i \in [n]} |a_i| \geq \sqrt{8 \log n}\right] \leq \frac{2}{n}.$$

□

Corollary 2. *Let $p, q \geq 0$ such that $p + q = 4$. Consider Gaussian random vectors $\boldsymbol{x}_i \in \mathbb{R}^d, i \in [n]$ such that $x_{ij} \underset{iid}{\sim} \mathcal{N}(0, 1), \forall i \in [n], j \in [d]$, and a fixed $\boldsymbol{z} \in \mathbb{R}^d$ such that $\|\boldsymbol{z}\| = 1$. Then,*

$$\max_{i \in [n]} \left|\langle \boldsymbol{x}_i, \boldsymbol{z}\rangle^p x_{ij}^q\right| \leq 64 \log^2 n$$

with probability at least $1 - \mathcal{O}(\frac{1}{n})$.

Proof. The result follows by noting that $\langle \boldsymbol{x}_i, \boldsymbol{z}\rangle \sim \mathcal{N}(0, 1)$ and $\left|\langle \boldsymbol{x}_i, \boldsymbol{z}\rangle^p x_{ij}^q\right| = |\langle \boldsymbol{x}_i, \boldsymbol{z}\rangle|^p |x_{ij}|^q$. □

Corollary 3. *Consider the following event defined using the notations from Corollary 2:*

$$\mathfrak{A} := \left\{\max_{i \in [n]} \left|\langle \boldsymbol{x}_i, \boldsymbol{z}\rangle^p x_{ij}^q\right| \leq 64 \log^2 n\right\}.$$

Then for any event $\mathfrak{B}$,

$$\mathbb{P}[\mathfrak{B}] \leq \mathbb{P}[\mathfrak{B} \mid \mathfrak{A}] + \mathcal{O}\left(\frac{1}{n}\right).$$

Proof. Note that

$$\mathbb{P}[\mathfrak{B}] = \mathbb{P}[\mathfrak{B} \mid \mathfrak{A}] \, \mathbb{P}[\mathfrak{A}] + \mathbb{P}[\mathfrak{B} \mid \neg\mathfrak{A}] \, \mathbb{P}[\neg\mathfrak{A}]$$

$$\leq \mathbb{P}[\mathfrak{B} \mid \mathfrak{A}] + \mathcal{O}\left(\frac{1}{n}\right)$$

□

Lemma 7. *Let $p, q \geq 0$ such that $p + q = 4$. Consider Gaussian random vectors $\boldsymbol{x}_i \in \mathbb{R}^d, i \in [n]$ such that $x_{ij} \underset{iid}{\sim} \mathcal{N}(0, 1), \forall i \in [n], j \in [d]$. Then, $\forall \boldsymbol{z} \in \mathbb{R}^d$ such that $\|\boldsymbol{z}\| = 1$ and for any $t > 0$,*

$$\mathbb{P}\left[\left|\frac{1}{n}\sum_{i=1}^{n}\langle\boldsymbol{x}_i, \boldsymbol{z}\rangle^p x_{i1}^q - \mathbb{E}\left[\frac{1}{n}\sum_{i=1}^{n}\langle\boldsymbol{x}_i, \boldsymbol{z}\rangle^p x_{i1}^q\right]\right| \geq t\right] \leq 2\exp\left(-\frac{nt^2}{C\log^4 n} + Dd\right) + \mathcal{O}\left(\frac{1}{n}\right),$$

for a sufficiently large absolute constants $C, D > 0$.

Proof. Consider a fixed $\boldsymbol{z} \in \mathbb{R}^d$ such that $\|\boldsymbol{z}\| = 1$. Let $\mathfrak{A}$ be the event defined in Corollary 3. Then using the result from Corollary 3,

$$\mathbb{P}\left[\left|\frac{1}{n}\sum_{i=1}^{n}\langle\boldsymbol{x}_i, \boldsymbol{z}\rangle^p x_{i1}^q - \mathbb{E}\left[\frac{1}{n}\sum_{i=1}^{n}\langle\boldsymbol{x}_i, \boldsymbol{z}\rangle^p x_{i1}^q\right]\right| \geq t\right] \leq \mathbb{P}\left[\left|\frac{1}{n}\sum_{i=1}^{n}\langle\boldsymbol{x}_i, \boldsymbol{z}\rangle^p x_{i1}^q - \mathbb{E}\left[\frac{1}{n}\sum_{i=1}^{n}\langle\boldsymbol{x}_i, \boldsymbol{z}\rangle^p x_{i1}^q\right]\right| \geq t \,\Big|\, \mathfrak{A}\right] + \mathcal{O}\left(\frac{1}{n}\right).$$
$$\tag{11}$$

Using Hoeffding inequality (Hoeffding, 1994) for the bounded-random variables:

$$\mathbb{P}\left[\left|\frac{1}{n}\sum_{i=1}^{n}\langle\boldsymbol{x}_i, \boldsymbol{z}\rangle^p x_{i1}^q - \mathbb{E}\left[\frac{1}{n}\sum_{i=1}^{n}\langle\boldsymbol{x}_i, \boldsymbol{z}\rangle^p x_{i1}^q\right]\right| \geq t \,\Big|\, \mathfrak{A}\right] \leq 2\exp\left(-\frac{nt^2}{C\log^4 n}\right),\tag{12}$$

where $C > 0$ is an absolute constant. Equation (12) holds for a fixed $\boldsymbol{z}$. We can extend these to hold for any $\boldsymbol{z} \in \mathbb{R}^d$ such that $\|\boldsymbol{z}\| = 1$ by using an ε-net argument and using a union bound across $\mathcal{O}(2^d)$ points in the net. Therefore, $\forall \boldsymbol{z} \in \mathbb{R}^d$ such that $\|\boldsymbol{z}\| = 1$ and for any $t > 0$:

$$\mathbb{P}\left[\left|\frac{1}{n}\sum_{i=1}^{n}\langle\boldsymbol{x}_i, \boldsymbol{z}\rangle^p x_{i1}^q - \mathbb{E}\left[\frac{1}{n}\sum_{i=1}^{n}\langle\boldsymbol{x}_i, \boldsymbol{z}\rangle^p x_{i1}^q\right]\right| \geq t \,\Big|\, \mathfrak{A}\right] \leq 2\exp\left(-\frac{nt^2}{C\log^4 n} + Dd\right),\tag{13}$$

where $D > 0$ is a sufficiently large constant. We complete the proof by combining the results from (11) and (13). □

Lemma 8. *Let $p, q \geq 0$ such that $p + q = 4$ and $p \in \{2, 3, 4\}$. Consider Gaussian random vectors $\boldsymbol{x}_i \in \mathbb{R}^d, i \in [n]$ such that $x_{ij} \underset{iid}{\sim} \mathcal{N}(0, 1), \forall i \in [n], j \in [d]$. Then, $\forall \boldsymbol{z} \in \mathbb{R}^d$ such that $\|\boldsymbol{z}\| = 1$,*

$$\mathbb{E}\left[\frac{1}{n}\sum_{i=1}^{n}\langle\boldsymbol{x}_i, \boldsymbol{z}\rangle^p x_{i1}^q\right] = C_{pq},$$

where $C_{pq} > 0$ is an absolute constant.

Proof. The result follows from a straightforward verification using bounded moments of Gaussian random variables. □

Next part of our analysis establishes concentration results for sets of covariates $\boldsymbol{x}_i$'s of sizes $(1-\epsilon)n$ and ϵn. The core idea of our approach is inspired by the methodology outlined in the work of Jambulapati et al. (2020).

Lemma 9. *Consider Gaussian random vectors $\boldsymbol{x}_i \in \mathbb{R}^d$ for $i \in [n]$, where each $x_{ij} \underset{iid}{\sim} \mathcal{N}(0, 1)$ for all $i \in [n]$ and $j \in [d]$. Let $p, q \geq 0$ such that $p + q = 4$ with $p \in \{2, 3, 4\}$. For any unit vector $\boldsymbol{z} \in \mathbb{R}^d$ (i.e., $|\boldsymbol{z}| = 1$), and for any $0 < \epsilon < \frac{1}{2}, \delta > 0$, and subset $S \subseteq [n]$ with $|S| = (1-\epsilon)n$, provided that $n = \Omega\left(\frac{d + \log\frac{1}{\delta}}{\epsilon^2\log\frac{1}{\epsilon}}\right)$, the following result holds:*

$$\mathbb{P}\left[\left|\frac{1}{(1-\epsilon)n}\sum_{i \in S}\langle\boldsymbol{x}_i, \boldsymbol{z}\rangle^p x_{i1}^q - C_{pq}\right| \geq \epsilon\sqrt{\log\frac{1}{\epsilon}}\log^2(\epsilon n)\right] \leq \mathcal{O}(\delta) + \mathcal{O}\left(\frac{1}{n}\right).$$

Proof. For any fixed $S \subseteq [n]$ such that $|S| = (1-\epsilon)n$,

$$\frac{1}{(1-\epsilon)n}\sum_{i \in S}\langle\boldsymbol{x}_i, \boldsymbol{z}\rangle^p x_{i1}^q = \frac{1}{1-\epsilon}\left(\frac{1}{n}\sum_{i=1}^{n}\langle\boldsymbol{x}_i, \boldsymbol{z}\rangle^p \boldsymbol{x}_{i1}^q\right) - \frac{\epsilon}{1-\epsilon}\left(\frac{1}{\epsilon n}\sum_{i \in [n]\setminus S}\langle\boldsymbol{x}_i, \boldsymbol{z}\rangle^p x_{i1}^q\right)\tag{14}$$

Following the result from Lemma 7,

$$\mathbb{P}\left[\left|\frac{1}{n}\sum_{i=1}^{n}\langle\boldsymbol{x}_i,\boldsymbol{z}\rangle^p x_{i1}^q - C_{pq}\right| \geq t\right] \leq 2\exp\left(\frac{-nt^2}{D_1\log^4 n} + D_2 d\right) + \mathcal{O}\left(\frac{1}{n}\right),$$

for some absolute constants $D_1, D_2 > 0$. We take $t = \frac{1-\epsilon}{2}\epsilon\sqrt{\log\frac{1}{\epsilon}}\log^2(\epsilon n)$ and $n = \Omega\left(\frac{d+\log\frac{1}{\delta}}{\epsilon^2\log\frac{1}{\epsilon}}\right)$. This leads to,

$$\mathbb{P}\left[\left|\frac{1}{n}\sum_{i=1}^{n}\langle\boldsymbol{x}_i,\boldsymbol{z}\rangle^p x_{i1}^q - C_{pq}\right| \geq \frac{1-\epsilon}{2}\epsilon\sqrt{\log\frac{1}{\epsilon}}\log^2(\epsilon n)\right] \leq \frac{\delta}{2} + \mathcal{O}\left(\frac{1}{n}\right), \tag{15}$$

Similarly, we can show that for some absolute constant $D_3, D_4 > 0$:

$$\mathbb{P}\left[\left|\frac{1}{\epsilon n}\sum_{i\in[n]\setminus S}\langle\boldsymbol{x}_i,\boldsymbol{z}\rangle^p x_{i1}^q - C_{pq}\right| \geq t \,\Bigg|\, \mathfrak{A}\right] \leq 2\exp\left(\frac{-\epsilon nt^2}{D_3\log^4(\epsilon n)} + D_4 d\right), \tag{16}$$

where the event $\mathfrak{A}$ is defined in Corollary 3. We need (16) to hold across any choice of $S \subseteq [n]$. Thus, we take a union bound across $\binom{n}{\epsilon n}$ choices. Note that $\log\binom{n}{\epsilon n} \leq n\epsilon\log\frac{1}{\epsilon}$. Therefore, for any choice of $S \subseteq [n]$,

$$\mathbb{P}\left[\left|\frac{1}{\epsilon n}\sum_{i\in[n]\setminus S}\langle\boldsymbol{x}_i,\boldsymbol{z}\rangle^p x_{i1}^q - C_{pq}\right| \geq t \,\Bigg|\, \mathfrak{A}\right] \leq 2\exp\left(\frac{-\epsilon nt^2}{D_3\log^4(\epsilon n)} + D_4 d + n\epsilon\log\frac{1}{\epsilon}\right),$$

We take $t = \frac{1-\epsilon}{2}\sqrt{\log\frac{1}{\epsilon}}\log^2(\epsilon n)$ and $n = \Omega\left(\frac{d+\log\frac{1}{\delta}}{\epsilon^2\log\frac{1}{\epsilon}}\right)$ and this leads to

$$\mathbb{P}\left[\left|\frac{1}{\epsilon n}\sum_{i\in[n]\setminus S}\langle\boldsymbol{x}_i,\boldsymbol{z}\rangle^p x_{i1}^q - C_{pq}\right| \geq \frac{1-\epsilon}{2}\sqrt{\log\frac{1}{\epsilon}}\log^2(\epsilon n) \,\Bigg|\, \mathfrak{A}\right] \leq \frac{\delta}{2}. \tag{17}$$

Following Corollary 3, and substituting the results of (15) and (17) in (14), we get

$$\mathbb{P}\left[\left|\frac{1}{(1-\epsilon)n}\sum_{i\in S}\langle\boldsymbol{x}_i,\boldsymbol{z}\rangle^p x_{i1}^q - C_{pq}\right| \geq \epsilon\sqrt{\log\frac{1}{\epsilon}}\log^2(\epsilon n)\right] \leq \mathcal{O}(\delta) + \mathcal{O}\left(\frac{1}{n}\right).$$

$\square$

Lemma 10. *Adopting the notation from Lemma 9, and for any choice of $0 < \epsilon < \frac{1}{2}$, $\delta > 0$, and $S \subseteq [n]$ such that $|S| = (1-\epsilon)n$ and $n = \Omega\left(\frac{d+\log\frac{1}{\delta}}{\epsilon^2\log\frac{1}{\epsilon}}\right)$, the following result holds:*

$$\left|\frac{1}{n}\sum_{i\in[n]\setminus S}\langle\boldsymbol{x}_i,\boldsymbol{z}\rangle^p x_{i1}^q\right| \leq \mathcal{O}\left(\epsilon\sqrt{\log\frac{1}{\epsilon}}\log^2(\epsilon n)\right)$$

with probability at least $1 - \mathcal{O}\left(\frac{1}{n}\right) - \mathcal{O}(\delta)$.

Proof. The result follows from the result of Lemma 9.

$$\frac{1}{n}\sum_{i\in[n]\setminus S}\langle\boldsymbol{x}_i,\boldsymbol{z}\rangle^p x_{i1}^q = \frac{1}{n}\sum_{i\in[n]}\langle\boldsymbol{x}_i,\boldsymbol{z}\rangle^p x_{i1}^q - \frac{1}{n}\sum_{i\in S}\langle\boldsymbol{x}_i,\boldsymbol{z}\rangle^p x_{i1}^q$$

$$= \frac{1}{n}\sum_{i\in[n]}\langle\boldsymbol{x}_i,\boldsymbol{z}\rangle^p x_{i1}^q - (1-\epsilon)\frac{1}{(1-\epsilon)n}\sum_{i\in S}\langle\boldsymbol{x}_i,\boldsymbol{z}\rangle^p x_{i1}^q$$

$$= \frac{1}{n}\sum_{i\in[n]}\langle\boldsymbol{x}_i,\boldsymbol{z}\rangle^p x_{i1}^q - C_{pq}$$

$$\quad - \left((1-\epsilon)\frac{1}{(1-\epsilon)n}\sum_{i\in S}\langle\boldsymbol{x}_i,\boldsymbol{z}\rangle^p x_{i1}^q - C_{pq}\right)$$

$$\left|\frac{1}{n}\sum_{i\in[n]\setminus S}\langle\boldsymbol{x}_i,\boldsymbol{z}\rangle^p x_{i1}^q\right| \leq \left|\frac{1}{n}\sum_{i\in[n]}\langle\boldsymbol{x}_i,\boldsymbol{z}\rangle^p x_{i1}^q - C_{pq}\right| + (1-\epsilon)\left|\left(\frac{1}{(1-\epsilon)n}\sum_{i\in S}\langle\boldsymbol{x}_i,\boldsymbol{z}\rangle^p x_{i1}^q - C_{pq}\right)\right| + \epsilon|C_{pq}|$$

$$\leq \mathcal{O}\left(\epsilon\sqrt{\log\frac{1}{\epsilon}}\log^2(\epsilon n)\right)$$

with probability at least $1 - \mathcal{O}\left(\frac{1}{n}\right) - \mathcal{O}\left(\delta\right)$. □

C Proof of Proposition 1

Proposition 1 (Impossibility with constant corruption proportion). *If the measurements follow the data generation process* (3) *with a corruption proportion $\epsilon > 0$, then for any estimator $\hat{\boldsymbol{\theta}}$ and any $\delta > 0$:*

$$\mathbb{P}\big[d(\hat{\boldsymbol{\theta}}, \boldsymbol{\theta}^*) \geq \delta\big] \geq \frac{\epsilon}{2} \ .$$

Proof. We show that proof in one dimension as an extension to d-dimension is straightforward. We consider the following phase retrieval model:

$$y = (x\theta)^2 + \eta_{\theta,x}$$

where $\eta_{\theta,x}$ denotes the adversarial corruption added by a strong adversary who has access to both x and θ. We draw x from a standard normal distribution. Consider two parameters $\theta_1 > 0$ and $\theta_2 > 0$ with $|\theta_1 - \theta_2| > \delta$ for some $\delta > 0$.

Let $D_1(x, y)$ and $D_2(x, y)$ be distributions over $\mathbb{R} \times \mathbb{R}$ corresponding to quadratic models $y = (x\theta_1)^2 + \eta_{\theta_1,x}$ and $y = (x\theta_2)^2 + \eta_{\theta_2,x}$ respectively. Since the adversary can only change ϵ fraction of inputs, we assume the following conditional distribution for y conditioned on x for $i \in \{1, 2\}$ for some $\sigma > 0$:

$$D_i(y|x) = \begin{cases} 1 - \epsilon, & \text{when } y = (x\theta_i)^2 \\ \frac{\epsilon}{\sigma}, & \text{when } y \in [\sigma, 2\sigma] \\ 0, & \text{otherwise} \end{cases}$$

We want to be able to differentiate between D_1 and D_2 based on the measurements (x, y) drawn from either D_1 or D_2. By reduction to a hypothesis testing problem and using the Neyman–Pearson lemma:

$$\inf_{\hat{\theta}} \sup_{\theta \in \{\theta_1, \theta_2\}} \mathbb{P}_\theta\big[|\hat{\theta} - \theta| > \delta\big] \geq \frac{1}{2}(1 - \text{TV}(D_1, D_2))$$

where $\text{TV}(D_1, D_2)$ is the total variation distance between distributions D_1 and D_2. Next, we compute an upper bound on $\text{TV}(D_1, D_2)$.

$$\begin{aligned} \text{TV}(D_1, D_2) &= \frac{1}{2} \int_{\mathbb{R} \times \mathbb{R}} |D_1(x, y) - D_2(x, y)| \, \mathrm{d}x \, \mathrm{d}y \\ &= \frac{1}{2} \int_{\mathbb{R} \times \mathbb{R}} D_1(x)|D_1(y|x) - D_2(y|x)| \, \mathrm{d}x \, \mathrm{d}y \end{aligned}$$

Notice that $D_1(y|x)$ and $D_2(y|x)$ can only differ when $(x\theta_1)^2 \neq (x\theta_2)^2$ and contribute $|D_1(y|x) - D_2(y|x)| \leq 2(1 - \epsilon)$ correspondingly. Overall,

$$\text{TV}(D_1, D_2) \leq 1 - \epsilon$$

It follows that,

$$\inf_{\hat{\theta}} \sup_{\theta \in \{\theta_1, \theta_2\}} \mathbb{P}_\theta\big[|\hat{\theta} - \theta| > \delta\big] \geq \frac{\epsilon}{2} \ .$$

□

D Constructing LSQ-PHASE-ORACLE and Proof of Theorem 2

In this section, we analyze the behavior of the loss function in (2) in the presence of corruption. Our discussion is framed within the context of Assumption 1, where we assume that the corruption η_i in the response y_i is independent of the covariates $\boldsymbol{x}_i$. For this part of the analysis, by possibly reindexing the measurements, we define

$$f_U(\boldsymbol{\theta}) = \frac{1}{4m} \sum_{i=1}^{m} \left(\langle \boldsymbol{x}_i, \boldsymbol{\theta}\rangle^2 - \langle \boldsymbol{x}_i, \boldsymbol{\theta}^*\rangle^2 - \eta_i\right)^2$$

$$\nabla f_U(\boldsymbol{\theta}) = \frac{1}{m} \sum_{i=1}^{m} \left(\langle \boldsymbol{x}_i, \boldsymbol{\theta}\rangle^2 - \langle \boldsymbol{x}_i, \boldsymbol{\theta}^*\rangle^2 - \eta_i\right)\boldsymbol{x}_i\boldsymbol{x}_i^\top\boldsymbol{\theta}$$

$$\nabla^2 f_U(\boldsymbol{\theta}) = \frac{1}{m} \sum_{i=1}^{m} \left(3\langle \boldsymbol{x}_i, \boldsymbol{\theta}\rangle^2 - \langle \boldsymbol{x}_i, \boldsymbol{\theta}^*\rangle^2 - \eta_i\right)\boldsymbol{x}_i\boldsymbol{x}_i^\top \ .$$

Note that up to k out of m measurements may have corrupted responses y_i. Without loss of generality, we assume that $\boldsymbol{\theta}^* = [1, 0, \ldots, 0]^\top$. Taking the expectation over $\boldsymbol{x}_1, \ldots, \boldsymbol{x}_m$, we derive the following expected quantities:

$$F_U(\boldsymbol{\theta}) = \frac{1}{4}\left(3\|\boldsymbol{\theta}\|^4 + 3 - 4\langle\boldsymbol{\theta}, \boldsymbol{\theta}^*\rangle^2 - 2\|\boldsymbol{\theta}\|^2 - 2\|\boldsymbol{\theta}\|^2\bar{\eta} + 2\bar{\eta} + \frac{1}{m}\sum_{i=1}^m \eta_i^2\right)$$

$$\nabla F_U(\boldsymbol{\theta}) = (3\|\boldsymbol{\theta}\|^2 - 1)\boldsymbol{\theta} - 2\langle\boldsymbol{\theta}, \boldsymbol{\theta}^*\rangle\boldsymbol{\theta}^* - \bar{\eta}\boldsymbol{\theta}$$

$$\nabla^2 F_U(\boldsymbol{\theta}) = 6\boldsymbol{\theta}\boldsymbol{\theta}^\top + 3\|\boldsymbol{\theta}\|^2 - I - 2\boldsymbol{\theta}^*\boldsymbol{\theta}^{*\top} - \bar{\eta}I \,,$$

where $\bar{\eta} = \frac{1}{m}\sum_{i=1}^m \eta_i$.

D.1 Geometry of F_U

Sun et al. (2018) investigated the geometry of the expected loss function in the absence of corruption. We extend this analysis to show that when the η_i's are independent of the $\boldsymbol{x}_i$'s, the geometry of $F_U(\boldsymbol{\theta})$ also exhibits a benign structure. This is formalized by characterizing the critical points of $F_U(\boldsymbol{\theta})$. At critical points,

$$\nabla F_U(\boldsymbol{\theta}) = \mathbf{0}$$

$$(3\|\boldsymbol{\theta}\|^2 - 1)\boldsymbol{\theta} - 2\langle\boldsymbol{\theta}, \boldsymbol{\theta}^*\rangle\boldsymbol{\theta}^* - \bar{\eta}\boldsymbol{\theta} = \mathbf{0} \,.$$

We end up with three possible scenarios:

1. $\boldsymbol{\theta} = \mathbf{0}$ is always a stationary point, but it behaves differently for different amount of average corruption.
   (a) When $\bar{\eta} \geq -1$, $\mathbf{0}$ is the local maxima (technically, it can also be considered a strict saddle point).
   (b) When $-3 < \bar{\eta} < -1$, $\mathbf{0}$ is a strict saddle point.
   (c) When $\bar{\eta} \leq -3$, $\mathbf{0}$ becomes the local (also global) minima due to the convexity of the $F_U(\boldsymbol{\theta})$.

2. When $\bar{\eta} \geq -1$, we can characterize a second set of critical points by a set

$$\mathcal{X} = \left\{\boldsymbol{\theta} \,\middle|\, 3\|\boldsymbol{\theta}\|^2 - 1 - \bar{\eta} = 0, \, \boldsymbol{\theta}^{*\top}\boldsymbol{\theta} = 0\right\} \,. \tag{18}$$

   They lead to strict saddle points.

3. Finally, when $\bar{\eta} \geq -3$, we get another set of critical points.

$$\mathcal{X}^* = \left\{\boldsymbol{\theta} \,\middle|\, \boldsymbol{\theta} = \pm\sqrt{1 + \frac{\bar{\eta}}{3}}\boldsymbol{\theta}^*\right\} \,. \tag{19}$$

   The points in $\mathcal{X}^*$ are the local (and global) minima.

Notably, all critical points of $F_U(\boldsymbol{\theta})$ are either strict saddle points or global minima. This suggests that the algorithms discussed in Section 2 are applicable for solving problem 2, even in the presence of corrupted measurements. For our analysis, we employed gradient descent with random initialization, as proposed by Chen et al. (2019).

D.2 Gradient descent updates with F_U

To gain intuition, we can study the dynamics of gradient descent with the (rather unrealistic) assumption that the gradient descent iterates $\tilde{\boldsymbol{\theta}}^t$ are independent of covariates $\boldsymbol{x}_i, i \in [m]$. This leads to the following update rule:

$$\tilde{\boldsymbol{\theta}}^{t+1} = \tilde{\boldsymbol{\theta}}^t - \mu(3\|\boldsymbol{\theta}\|^2 - 1)\boldsymbol{\theta} - 2\langle\boldsymbol{\theta}, \boldsymbol{\theta}^*\rangle\boldsymbol{\theta}^* - \bar{\eta}\boldsymbol{\theta} \tag{20}$$

where $\mu > 0$ is the chosen step size. We define the following two quantities:

$$\alpha_t = \tilde{\theta}_1^t, \quad \beta_t = \sqrt{\sum_{i=2}^d (\tilde{\theta}_i^t)^2} \tag{21}$$

Without loss of generality, we can assume that $\alpha_0 > 0$. Equation (20) leads to following dynamics for α_t and β_t:

$$\alpha_{t+1} = \left(1 + \mu\big(3 + \bar{\eta} - 3(\alpha_t^2 + \beta_t^2)\big)\right)\alpha_t \tag{22}$$

$$\beta_{t+1} = \left(1 + \mu\big(1 + \bar{\eta} - 3(\alpha_t^2 + \beta_t^2)\big)\right)\beta_t$$

We observe that (22) has three fixed points (α, β):

1. $(\alpha, \beta) = (0, 0)$ corresponds to $\boldsymbol{\theta} = \boldsymbol{0}$.

2. When $\bar{\eta} \geq -1$, then $(\alpha, \beta) = (0, \sqrt{\frac{1+\bar{\eta}}{3}})$ corresponds to points in $\mathcal{X}$, defined in (18).

3. When $\bar{\eta} \geq -3$, then $(\alpha, \beta) = (\sqrt{1 + \frac{\bar{\eta}}{3}}, 0)$ corresponds to points in $\mathcal{X}^*$, defined in (19).

In the absence of corruption, Chen et al. (2019) developed a "leave-one-out" technique to demonstrate that an approximately similar dynamic to (22) can be achieved using updates based on $f_U(\boldsymbol{\theta})$, despite the gradient descent iterates $\tilde{\boldsymbol{\theta}}^t$ being dependent on the covariates $\boldsymbol{x}_i$ for all $i \in [m]$. This framework is also applicable to our setting.

D.3 Proof Sketch for Theorem 2

In this subsection, we outline the key proof ideas for Theorem 2. The proof builds directly on the approach used in Theorem 2 of Chen et al. (2019), allowing us to focus on the novel aspects that differentiate our work from theirs. Full details are omitted here to highlight the distinctions.

Consider the following dynamics for α_t and β_t defined in (21):

$$\alpha_{t+1} = \left(1 + \mu\big(3 + \bar{\eta} - 3(\alpha_t^2 + \beta_t^2)\big) + \mu\zeta_t\right)\alpha_t , \tag{23}$$

$$\beta_{t+1} = \left(1 + \mu\big(1 + \bar{\eta} - 3(\alpha_t^2 + \beta_t^2)\big) + \mu\rho_t\right)\beta_t ,$$

where ζ_t and ρ_t are the perturbation terms. Next, we discuss the major parts of the proof.

D.3.1 When f_U is convex

The first part deals with the case when $\bar{\eta} < -3$. In this scenario, $f_U(\boldsymbol{\theta})$ can be shown to be a convex function with high probability. To that end, we prove the following result.

Lemma 11. *Let* $n = \Omega\big(\frac{d \operatorname{polylog}(d) + \log(\frac{1}{\delta})}{\epsilon^2 \log(\frac{1}{\epsilon})}\big)$ *and* $k \in \mathcal{K}$. *If* $\bar{\eta} = -3 - \varepsilon$ *for some* $\varepsilon > 0$, *then* $f_U(\boldsymbol{\theta})$ *is a convex function with probability at least* $1 - \delta - \mathcal{O}\big(\frac{1}{n}\big)$.

Proof. We proceed with studying the spectral properties of $\nabla^2 f_U(\boldsymbol{\theta})$. We want to show that $\nabla^2 f_U(\boldsymbol{\theta}) \succeq 0$ with high probability. Recall that

$$\nabla^2 f_U(\boldsymbol{\theta}) = \frac{1}{m}\sum_{i=1}^m \left(3\langle \boldsymbol{x}_i, \boldsymbol{\theta}\rangle^2 - \langle \boldsymbol{x}_i, \boldsymbol{\theta}^*\rangle^2 - \eta_i\right)\boldsymbol{x}_i\boldsymbol{x}_i^\top$$

For any $\boldsymbol{z} \in \mathbb{R}^d$ such that $\|\boldsymbol{z}\| = 1$,

$$\boldsymbol{z}^\top \nabla^2 f_U(\boldsymbol{\theta})\boldsymbol{z} = \boldsymbol{z}^\top \nabla^2 f_U(\boldsymbol{\theta})\boldsymbol{z} - \boldsymbol{z}^\top \nabla^2 F_U(\boldsymbol{\theta})\boldsymbol{z} + \boldsymbol{z}^\top \nabla^2 F_U(\boldsymbol{\theta})\boldsymbol{z} .$$

Observe that,

$$\boldsymbol{z}^\top \nabla^2 f_U(\boldsymbol{\theta})\boldsymbol{z} = \frac{1}{m}\sum_{i=1}^m \left(3\langle \boldsymbol{x}_i, \boldsymbol{\theta}\rangle^2\langle \boldsymbol{x}_i, \boldsymbol{z}\rangle^2 - \langle \boldsymbol{x}_i, \boldsymbol{\theta}^*\rangle^2\langle \boldsymbol{x}_i, \boldsymbol{z}\rangle^2 - \eta_i\langle \boldsymbol{x}_i, \boldsymbol{z}\rangle^2\right)$$

$$= \frac{1}{m}\sum_{i=1}^m \left(3\langle \boldsymbol{x}_i, \boldsymbol{\theta}\rangle^2\langle \boldsymbol{x}_i, \boldsymbol{z}\rangle^2 - x_{i1}^2\langle \boldsymbol{x}_i, \boldsymbol{z}\rangle^2 - \eta_i\langle \boldsymbol{x}_i, \boldsymbol{z}\rangle^2\right) .$$

and,

$$\boldsymbol{z}^\top \nabla^2 F_U(\boldsymbol{\theta})\boldsymbol{z} = 6\langle \boldsymbol{\theta}, \boldsymbol{z}\rangle^2 + 3\|\boldsymbol{\theta}\|^2 - 1 - 2z_1^2 - \bar{\eta} .$$

Using Lemma 14 from (Chen et al., 2019), if $n = \Omega(d \operatorname{polylog}(d))$, then for some absolute constant $c_0 > 0$, the following results hold with probability at least $1 - \mathcal{O}(n^{-10})$:

$$\frac{1}{m}\sum_{i=1}^m \left(3\langle \boldsymbol{x}_i, \boldsymbol{\theta}\rangle^2\langle \boldsymbol{x}_i, \boldsymbol{z}\rangle^2 - 6\langle \boldsymbol{\theta}, \boldsymbol{z}\rangle^2 - 3\|\boldsymbol{\theta}\|^2\right) \geq -c_0\sqrt{\frac{d\log^3 m}{m}}\|\boldsymbol{\theta}\|^2$$

$$\frac{1}{m}\sum_{i=1}^m \left(x_{i1}^2\langle \boldsymbol{x}_i, \boldsymbol{z}\rangle^2 - 1 - 2z_1^2\right) \geq -c_0\sqrt{\frac{d\log^3 m}{m}}$$

Next, notice that $\eta_i \langle \boldsymbol{x}_i, \boldsymbol{z} \rangle$ is a subexponential random variable with parameters $(2\eta_i, 4\eta_i)$. Using the Bernstein-type inequality (Vershynin, 2010), we can write:

$$\mathbb{P}\left[\left|\frac{1}{m}\sum_{i=1}^{m}\left(\eta_i\langle\boldsymbol{x}_i,\boldsymbol{z}\rangle^2 - \eta_i\right)\right| \geq 2t\max_{i\in[m]}|\eta_i|\right] \leq 2\exp\left(-cmt^2\right)$$

for some constant $c > 0$ and $t \in [0, 1]$. By taking, $t = \sqrt{\frac{d\log m}{m}}$ and using a covering argument similar to Chen et al. (2019), we can write $\forall \boldsymbol{z} \in \mathbb{R}^d$ and $\|\boldsymbol{z}\| = 1$,

$$\frac{1}{m}\sum_{i\in[m]}\left(\eta_i\langle\boldsymbol{x}_i,\boldsymbol{z}\rangle^2 - \eta_i\right) \geq -2\sqrt{\frac{d\log m}{m}}\max_{i\in U}|\eta_i|$$

with probability at least $1 - \mathcal{O}\left(\frac{1}{m}\right)$. Combining all the results, we have

$$\boldsymbol{z}^\top\nabla^2 f_U(\boldsymbol{\theta})\boldsymbol{z} \geq -c_0\sqrt{\frac{d\log^3 m}{m}}\|\boldsymbol{\theta}\|^2 - c_0\sqrt{\frac{d\log^3 m}{m}} - 2\sqrt{\frac{d\log m}{m}}\max_{i\in U}|\eta_i| + 6\langle\boldsymbol{\theta},\boldsymbol{z}\rangle^2 + 3\|\boldsymbol{\theta}\|^2 - 1 - 2z_1^2 - \bar{\eta}$$

$$\geq -c_0\sqrt{\frac{d\log^3 m}{m}}\|\boldsymbol{\theta}\|^2 - c_0\sqrt{\frac{d\log^3 m}{m}} - 2\sqrt{\frac{d\log m}{m}}\max_{i\in U}|\eta_i| + 3\|\boldsymbol{\theta}\|^2 + \varepsilon$$

By noticing that $\max_{i\in[m]}|\eta_i| = \mathcal{O}(\log n)$, $m = (1 - 2\epsilon)n$ and taking $n = \Omega(\frac{d\,\mathrm{polylog}(d)}{\varepsilon^2})$, we show that $\forall \boldsymbol{z} \in \mathbb{R}^d$ and with probability at least $1 - \delta - \mathcal{O}\left(\frac{1}{n}\right)$

$$\boldsymbol{z}^\top\nabla^2 f_U(\boldsymbol{\theta})\boldsymbol{z} \geq \frac{\varepsilon}{2}.$$

□

Moreover, the global minimum of $f_U(\boldsymbol{\theta})$ is attained at $\boldsymbol{0}$. Algorithm 3 leverages this property to return $\boldsymbol{0}$ when it estimates that the average corruption is less than -3. However, since the algorithm does not have direct access to the true value of $\bar{\eta}$, it requires a method to estimate the average corruption. For this purpose, we define the following quantity:

$$\kappa_{\mathrm{sq}} = \frac{1}{3|U|}\sum_{i\in U}\left(y_i z_i - (d-1)y_i\right),$$

where $z_i = \sum_{j=1}^{d} x_{ij}^2, \forall i \in [m]$.

In the remaining part of the proof sketch, we assume that $\bar{\eta} \geq -3$. Next, we show that κ_{sq} provides a good estimation of $1 - \frac{\bar{\eta}}{3}$ with high probability.

We discuss the setting of κ_{sq} below:

$$\kappa_{\mathrm{sq}} = \frac{1}{3}\left(\sqrt{2}\sqrt{\frac{1}{m}\sum_{i=1}^{m}y_i^2 - \left(\frac{1}{m}\sum_{i=1}^{m}y_i\right)^2} + \frac{1}{m}\sum_{i=1}^{m}y_i\right)$$

Note that

$$\frac{1}{m}\sum_{i=1}^{m}y_i^2 = \frac{1}{m}\sum_{i=1}^{m}\left(\langle\boldsymbol{x}_i,\boldsymbol{\theta}^*\rangle^4 + \eta_i^2 + 2\eta_i\langle\boldsymbol{x}_i,\boldsymbol{\theta}^*\rangle^2\right)$$

Using the same argument as Lemma 7 $\forall j \in [d]$,

$$\mathbb{P}\left[\left|\frac{1}{m}\sum_{i=1}^{m}\langle\boldsymbol{x}_i,\boldsymbol{\theta}^*\rangle^4 - \mathbb{E}\left[\frac{1}{m}\sum_{i=1}^{m}\langle\boldsymbol{x}_i,\boldsymbol{\theta}^*\rangle^4\right]\right| \geq \varepsilon\right] \leq 2\exp\left(-\frac{m\varepsilon^2}{C\log^4 m}\right) + \mathcal{O}\left(\frac{1}{m}\right),$$

Using the Bernstein-type inequality (Vershynin, 2010) for subexponential random variables $\eta_i \langle \boldsymbol{x}_i, \boldsymbol{\theta}^* \rangle^2, \forall i \in [m]$:

$$\mathbb{P}\left[\left|\frac{1}{m}\sum_{i=1}^{m}\left(\eta_i \langle \boldsymbol{x}_i, \boldsymbol{\theta}^* \rangle^2 - \eta_i\right)\right| \geq \varepsilon \max_{i \in [m]}|\eta_i|\right] \leq 2\exp\left(-cm\varepsilon^2\right) ,$$

for $\varepsilon \in (0,1)$ and some absolute constant $c > 0$. Similarly, $\frac{1}{m}\sum_{i=1}^{m}y_i$ concentrates sharply around $\|\boldsymbol{\theta}^*\|^2 + \bar{\eta}$. Combining the above results together, we can show that

$$\left(1 + \frac{\bar{\eta}}{3}\right) - \mathcal{O}\left(\varepsilon\right) \leq \kappa_{\mathrm{sq}} \leq \left(1 + \frac{\bar{\eta}}{3}\right) + \mathcal{O}\left(\varepsilon\right) + \mathcal{O}\left(\epsilon \log^2 m\right) ,$$

with probability at least $1 - \mathcal{O}\left(\delta\right) - \mathcal{O}\left(\frac{1}{m}\right)$.

D.3.2 When approximate dynamics for α_t and β_t holds

Following a similar line of reasoning as in Chen et al. (2019), the subsequent part of the proof demonstrates that if the dynamics in (23) hold for $\zeta_t = \mathcal{O}\left(\frac{1}{\log d}\right)$ and $\rho_t = \mathcal{O}\left(\frac{1}{\log d}\right)$, then there exists some $\nu \in (0,1)$ and a corresponding $T_0 = T_0(\nu) = \mathcal{O}\left(\log d\right)$ such that:

$$|\alpha_{T_0} - \kappa| \leq \frac{\nu}{2}, \quad \beta_{T_0} \leq \frac{\nu}{2} .$$

This result implies that $d(\tilde{\boldsymbol{\theta}}^{T_0}, \kappa\boldsymbol{\theta}^*) \leq \nu$. Achieving this bound relies on an effective initialization, which is attained by setting $\tilde{\boldsymbol{\theta}}^0 = \sqrt{\kappa_{\mathrm{sq}}}\boldsymbol{u}$, where $\boldsymbol{u}$ is uniformly distributed on the unit sphere. The arguments closely follow the reasoning presented in the proof of Theorem 3 in Chen et al. (2019).

D.3.3 Justification for approximate dynamics of α_t and β_t

Chen et al. (2019) employ a variant of leave-one-out arguments to demonstrate that the dynamics described in (23) hold, with $\zeta_t = \mathcal{O}\left(\frac{1}{\log d}\right)$ and $\rho_t = \mathcal{O}\left(\frac{1}{\log d}\right)$. Their approach is based on constructing three specific leave-one-out sequences: the l-th leave-one-out sequence, the random sign sequence, and the l-th leave-one-out with random sign sequence. These sequences are instrumental in establishing a form of *near-independence* between the iterates $\tilde{\boldsymbol{\theta}}^t$ and the covariates $\boldsymbol{x}_i$ for all $i \in [m]$. Below, we provide formal definitions of these four sequences of iterates (including the original sequence) and outline their respective update rules:

Original sequence: $\qquad \nabla f(\boldsymbol{\theta}) = \frac{1}{m}\sum_{i=1}^{m}\left(\langle \boldsymbol{x}_i, \boldsymbol{\theta}\rangle^2 - \langle \boldsymbol{x}_i, \boldsymbol{\theta}^*\rangle^2 - \eta_i\right)\boldsymbol{x}_i\boldsymbol{x}_i^\top\boldsymbol{\theta}$
$\qquad\qquad\qquad\qquad\qquad\qquad \tilde{\boldsymbol{\theta}}^{t+1} = \tilde{\boldsymbol{\theta}}^t - \mu\nabla f(\tilde{\boldsymbol{\theta}}^t)$

l-th leave-one-out sequence: $\qquad \nabla f^{(l)}(\boldsymbol{\theta}) = \frac{1}{m}\sum_{i=1,i\neq l}^{m}\left(\langle \boldsymbol{x}_i, \boldsymbol{\theta}\rangle^2 - \langle \boldsymbol{x}_i, \boldsymbol{\theta}^*\rangle^2 - \eta_i\right)\boldsymbol{x}_i\boldsymbol{x}_i^\top\boldsymbol{\theta}$
$\qquad\qquad\qquad\qquad\qquad\qquad \tilde{\boldsymbol{\theta}}^{t+1,(l)} = \tilde{\boldsymbol{\theta}}^{t,(l)} - \mu\nabla f^{(l)}(\tilde{\boldsymbol{\theta}}^{t,(l)})$

Random sign sequence: $\qquad \nabla f^{\mathrm{sgn}}(\boldsymbol{\theta}) = \frac{1}{m}\sum_{i=1}^{m}\left(\langle \boldsymbol{x}_i^{\mathrm{sgn}}, \boldsymbol{\theta}\rangle^2 - \langle \boldsymbol{x}_i^{\mathrm{sgn}}, \boldsymbol{\theta}^*\rangle^2 - \eta_i\right)\boldsymbol{x}_i^{\mathrm{sgn}}\boldsymbol{x}_i^{\mathrm{sgn}\top}\boldsymbol{\theta}$
$\qquad\qquad\qquad\qquad\qquad\qquad \tilde{\boldsymbol{\theta}}^{t+1,\mathrm{sgn}} = \tilde{\boldsymbol{\theta}}^{t,\mathrm{sgn}} - \mu\nabla f^{\mathrm{sgn}}(\tilde{\boldsymbol{\theta}}^{t,\mathrm{sgn}})$

l-th leave-one-out and random sign sequence: $\quad \nabla f^{(l),\mathrm{sgn}}(\boldsymbol{\theta}) = \frac{1}{m}\sum_{i=1,i\neq l}^{m}\left(\langle \boldsymbol{x}_i^{\mathrm{sgn}}, \boldsymbol{\theta}\rangle^2 - \langle \boldsymbol{x}_i^{\mathrm{sgn}}, \boldsymbol{\theta}^*\rangle^2 - \eta_i\right)\boldsymbol{x}_i^{\mathrm{sgn}}\boldsymbol{x}_i^{\mathrm{sgn}\top}\boldsymbol{\theta}$
$\qquad\qquad\qquad\qquad\qquad\qquad \tilde{\boldsymbol{\theta}}^{t+1,\mathrm{sgn},(l)} = \tilde{\boldsymbol{\theta}}^{t,\mathrm{sgn},(l)} - \mu\nabla f^{(l),\mathrm{sgn}}(\tilde{\boldsymbol{\theta}}^{t,\mathrm{sgn},(l)})$

The notations used here follow closely from Chen et al. (2019). Specifically, for a given $\boldsymbol{x}_i^{\mathrm{sgn}}$, we define $x_{ij}^{\mathrm{sgn}} = x_{ij}$ for $j \neq 1$ and $x_{i1}^{\mathrm{sgn}} = w_i x_{i1}$, where w_i is a Rademacher random variable. All sequences are initialized with $\tilde{\boldsymbol{\theta}}^0$, and a constant step size $\mu > 0$ is employed.

It is important to note that the analysis involves additional concentration inequalities due to the presence of corruption. Specifically, we need to ensure that the absence of terms such as $\mu\frac{1}{m}\boldsymbol{x}_l\boldsymbol{x}_l^\top\boldsymbol{\theta}^{t,(l)}$ does not cause the gradient $\nabla f^{(l)}(\boldsymbol{\theta})$ to deviate significantly from $\nabla f(\boldsymbol{\theta})$. We demonstrate that such deviations remain controlled, ensuring the robustness of the overall analysis.

$$\|\mu\frac{1}{m}\eta_i\boldsymbol{x}_l\boldsymbol{x}_l^\top\boldsymbol{\theta}^{t,(l)}\| \underset{(i)}{\lesssim} \mu\frac{1}{m}\log m\left|\boldsymbol{x}_l^\top\boldsymbol{\theta}^{t,(l)}\right|\|\boldsymbol{x}_l\|$$

$$\underset{(ii)}{\lesssim} \mu\frac{1}{m}\log m\sqrt{\log m}\|\boldsymbol{\theta}^{t,(l)}\|\sqrt{d}$$

$$\lesssim \mu\frac{\sqrt{d\log^3 m}}{m}\|\boldsymbol{\theta}^{t,(l)}\| .$$

In the above derivation, step (i) follows from the fact that $\eta_i = \mathcal{O}\left(\log m\right)$, while step (ii) leverages the tail bounds for the maximum of a standard Gaussian variable and the norm of a Gaussian vector. A similar reasoning applies to other corruption-related terms that emerge in the analysis. The rest of the analysis is similar to Chen et al. (2019).

E   Experimental Comparisons

We evaluated the performance of our method against established approaches for robust phase retrieval, specifically comparing with Median RWF (Zhang et al., 2016a) and PhaseLift (Hand, 2017). Median RWF employs spectral initialization, while PhaseLift relies on a convex SDP formulation. The covariates $\boldsymbol{x}_i$ were sampled from a standard normal distribution, and the corruption was uniformly distributed within the range $[-5, 5]$. We conducted experiments with $k = n^{\frac{2}{3}}$ and $n = 10d \log d$ for $d \in \{50, 500, 1000\}$. Algorithm 3 served as LSQ-PHASE-ORACLE in our method. All the first-order updates (inner loop in our method and gradient descent type updates in Median RWF) were run for 500 iterations. Performance metrics included relative error, defined as $\frac{d(\boldsymbol{\theta}, \boldsymbol{\theta}^*)}{\|\boldsymbol{\theta}^*\|}$, and runtime, with results averaged over 5 independent runs. All methods were implemented in MATLAB and tested on a MacBook Pro with macOS 14.4.1, 32 GB memory, and an Apple M2 Max chip. For PhaseLift, CVX was employed as the SDP solver, and experiments were manually terminated if no solution was found within 5 minutes.

Table 1: Comparison of the performance of different methods across various values of d. Runtime is measured in seconds, with all values rounded to three decimal places.

Method	$d = 50$		$d = 500$		$d = 1000$	
	Rel Error	Run time	Rel Error	Run time	Rel Error	Run time
ALT-MIN-PHASE	0.003 ± 0.002	0.553 ± 0.01	0.000 ± 0.000	13.060 ± 0.303	0.000 ± 0.000	56.519 ± 0.690
Median RWF	0.000 ± 0.000	0.404 ± 0.015	0.000 ± 0.000	24.907 ± 0.518	0.000 ± 0.000	139.219 ± 0.926
PhaseLift	0.000 ± 0.000	102.093 ± 6.945	NA	> 300	NA	> 300

For $d = 50$, all methods demonstrated comparable performance, though PhaseLift exhibited the highest runtime due to its SDP-based approach. As d increased, PhaseLift failed to produce results within the 5-minute threshold. For larger dimensions, $d \in \{500, 1000\}$, our method showed performance comparable to Median RWF in terms of relative error, but it significantly outperformed Median RWF in terms of runtime efficiency.